



MASTER SCIENCE DE LA MATIÈRE
École Normale Supérieure de Lyon
Université Claude Bernard Lyon I

Stage 2010–2011
Claire Lebouteiller
M1 Physique

Design and realization of magnetic coils for ultracold atoms experiments

Abstract : This report compiles information about the design and conception of magnetic coils able to create a strong and homogeneous magnetic field gradient on a 3D optical lattice trapping Bose-Einstein condensate of Rubidium atoms. This gradient, generated by two coils in an anti-Helmoltz configuration and directed by bias coils, reaches 30 Gauss/cm. It can be projected on any axis of the space thanks to six bias coils, two in each direction of the space, in a Helmoltz configuration. The purpose of this gradient is to enable experiments such as lattice tilt leading to anti-ferromagnetic phase ordering [1] [2] as well as spin gradient thermometry [3] [4] [5]. Numerical simulations of the magnetic field created have been carried out to maximize its gradient and to make sure the curvature will be low enough to not interfere with the trapping frequency of the optical lattice. A new design has been made to ensure optical access to the chamber and stability of the coils and optical elements surrounding them. The pair of coils creating the gradient have also been realized and characterized and verify the numerical simulations predictions.

Key words : Ultracold atoms, Magnetic coils, Helmoltz configuration, Optical lattice, Bose-Hubbard model.

Internship supervised by:

Pr. Wolfgang Ketterle

[ketterle\(at\)mit.edu](mailto:ketterle(at)mit.edu) / tel. 1-617-253-6815

Center for Ultracold Atoms (CUA),
Massachusetts Institute of Technology (MIT)
77 Massachusetts Avenue
Cambridge, MA02139, USA
http://cua.mit.edu/ketterle_group/



**Massachusetts
Institute of
Technology**



Acknowledgments

First of all, I wish to thank Wolfgang Ketterle for having me in his group and answering my questions. The hallway is an amazing place to learn physics. Then, I would like to thank the BEC IV team: David Weld, Georgios Siviloglou and Hiro Miyake for all their help and their advices, I really appreciate the time taken to explain me everything I needed to know. Of course come next all the other people which whom I shared the office and who made my time at MIT truly unforgettable, so thank you Ivana Dimitrova, Jesse Amato-Grill and Niklas Jepsen. And thanks as well to all the people in the hallway who contributed to this friendly atmosphere, Thomas Gersdorf, Thomas Rigaldo... and everybody else. I add a special thanks to my coil making slave.

Contents

1	Introduction	1
2	Theoretical introduction	1
2.1	Bose-Einstein condensate	1
2.2	Optical lattice	2
2.3	Cold atoms in an optical lattice	3
2.4	Prospective experiments	5
3	Simulation and requirement on the magnetic field	7
3.1	Magnetic fields and choice of the coils configuration	7
3.2	Numerical simulations	11
3.3	Requirement on the magnetic field	13
4	Construction and characterization of the coils	15
4.1	Choice of the wire	15
4.2	Final values for the parameters	16
4.3	Details about the construction	16
4.4	Characterization of the magnetic field in the science chamber	17
5	Conclusion	18
References		18
Appendices		20
A	Description of the apparatus for cooling	20
B	Gradient coils	22
B.1	Fabrication	22
B.2	Coils	23
C	Code to calculate the magnetic field	24

1 Introduction

Experimental progress in the past decades has enabled us to study the behavior of atoms at very low temperatures, on the order of nano-kelvins. An interesting feature of this new physics is trapping the atoms in an optical lattice, formed by interfering laser beams, and using this system as a condensed matter quantum simulator. Indeed, if condensed matter systems are constituted of nuclei and electrons whose mutual interactions are known, the periodic assembly of many of them leads to really complex systems which hard to study. Their collective behavior cannot always be predicted and explained because of the entanglement of many elements: Coulomb interaction, lattice vibration, lattice defects, charge fluctuation. As it is not possible to isolate and vary the parameters in a real crystal, it is therefore hard to know which cause leads to which effect. This is how the study of ultracold atoms, mimicking electrons, loaded into optical lattices whose potential is similar to the potential created by periodically spaced nuclei, comes into play. This artificial crystal of quantum matter offers perfect control over the lattice parameters such as the periodicity and lattice depth which can be respectively changed by varying the laser intensity and wavelength.

I took part to the BEC IV team which use a machine working with ultracold atoms of Rubidium 87 (=boson) in an optical lattice. Several kinds of experiments can be done with this machine and my work was to design new magnetic coils in order to obtain a strong and homogeneous magnetic field gradient in the science chamber, where the measurements are taken. This report will be divided as following. First, a broad introduction on the way to reach low temperatures, the behavior of atoms in optical lattices and the possible experiments on them will be given. Then, a second part will be dealing with the magnetic field and the way to simulate it, as well as the coils configuration and requirements. And finally, in the last part will be presented the technical details on the construction and the characterization of a pair of magnetic coils.

2 Theoretical introduction

2.1 Bose-Einstein condensate

At a critical phase space density, a classical dilute bosonic gas undergoes a phase transition leading to a quantum-degenerate Bose-Einstein condensate(BEC), so called after the name of the Indian physicist Bose who had the idea of treating photons as a gas of identical particles and Einstein who extended this idea to matter particles. This phenomenon usually occurs at very low temperature, when the distance d between two atoms in the gas becomes comparable to the De Broglie wavelength λ_B

$$\lambda_B = \sqrt{\frac{2\pi\hbar^2}{mk_B T}} \quad (1)$$

where \hbar is the reduced Plank constant, m the mass of the atom, k_B the Boltzmann constant and T the temperature. Then, the wave function of the atoms overlap and a macroscopic fraction of them condense into a giant matter wave. The atoms lose their individual nature and adopt a collective behavior. This happens only with bosons, that is to say particles with integer spin because the Pauli principle prevents two fermions of being in the same quantum state. One could expect rubidium atoms to form a solid at low temperature. However, an atomic thermal gas can be observed because of the really low density of atoms present in the cloud. This is a metastable state and after some time, the atoms will congregate to form a solid but as there are very few atoms, the collisions between them will not occur at a fast rate and experiments can be performed on the gas. The formation of molecules or aggregates requires at least three atoms very close to each other: two atoms colliding and forming a molecule and a third to take away the energy released by the molecule formation. At very low density, this proximity is unlikely, which is why molecules form very slowly, leaving time for experiments on gas.

Noninteracting Bose gas:

A noninteracting Bose gas is in a fully condensed state at zero temperature, that is to say all the N particles composing this gas are described by identical single particle wave functions. Consequently, the many body wave function can be expressed as the product of these identical single particle wave functions $\phi(\vec{r})$:

$$\Psi_N(\vec{r}_1, \vec{r}_2, \dots, \vec{r}_N) = \prod_{i=1}^N \phi(\vec{r}_i) \quad (2)$$

Defining the macroscopic wave function $\psi(\vec{r}) = \sqrt{N}\phi(\vec{r})$, the particle density is given by $n(\vec{r}) = |\phi(\vec{r})|^2$.

Interactions:

In a cold dilute gas (typical density between 10^{12} and 10^{15} atoms/cm³) only the two-body interactions need to be taken into account, as was mentioned previously. The true interaction between two atoms is complicated because attractive at long range and repulsive at short range. However, at very low temperature, since the thermal De Broglie wavelength is large compared to the details of the interaction potential, only the s-wave scattering process is relevant. Hence, the interaction potential can be described as an effective contact potential:

$$V_{int}(\vec{r}) = \frac{4\pi\hbar^2 a_s}{m} \cdot \delta(\vec{r}) = g \cdot \delta(\vec{r}), \quad (3)$$

where \vec{r} is the relative coordinate between the two interacting atoms, a_s is the s-wave scattering length, m is the mass of the atoms and $g = 4\pi\hbar^2 a_s/m$ is the coupling constant.

Weakly interacting Bosons:

The s-wave collisions mentioned above will add a non linear term to the normal Schrödinger equation. Therefore, a weakly interacting bosonic system confined in an external potential V_{ext} is described by the following many body Hamiltonian:

$$\hat{H} = \int \hat{\psi}^\dagger(\vec{r}) \left(-\frac{\hbar^2}{2m} \nabla^2 + V_{ext}(\vec{r}) \right) \hat{\psi}(\vec{r}) d\vec{r} + \frac{1}{2} \int \hat{\psi}^\dagger(\vec{r}) \hat{\psi}^\dagger(\vec{r}') V_{int}(\vec{r} - \vec{r}') \hat{\psi}(\vec{r}') \hat{\psi}(\vec{r}) d\vec{r} d\vec{r}' \quad (4)$$

$$\stackrel{(3)}{=} \int \hat{\psi}^\dagger(\vec{r}) \left(-\frac{\hbar^2}{2m} \nabla^2 + V_{ext}(\vec{r}) \right) \hat{\psi}(\vec{r}) d\vec{r} + \frac{4\pi\hbar^2 a_s}{2m} \int \hat{\psi}^\dagger(\vec{r}) \hat{\psi}^\dagger(\vec{r}') \hat{\psi}(\vec{r}') \hat{\psi}(\vec{r}) d\vec{r} \quad (5)$$

where $\hat{\psi}^\dagger(\vec{r})$ and $\hat{\psi}(\vec{r})$ are respectively the creation and annihilation field operators for bosons.

If the many-body state can be described by the macroscopic wavefunction $\psi(\vec{r})$, the previous hamiltonian 5 leads to the Gross-Pitaevski equation:

$$i\hbar \frac{\partial}{\partial t} \psi(\vec{r}, t) = \left(-\frac{\hbar^2}{2m} \nabla^2 + V_{ext}(\vec{r}) + g|\psi(\vec{r}, t)|^2 \right) \psi(\vec{r}, t), \quad (6)$$

which corresponds to the Schrödinger equation with an additional non-linear term due to the interactions.

2.2 Optical lattice

Optical dipole trap

Neutral atoms can be optically trapped due to the fact that a spatially varying light field $\vec{E}(\vec{r})$ induces an electric dipole moment \vec{d} in the atoms which modify their energy via the so-called AC Stark effect. In return, the induced dipole interacts with the light field, creating a dipole potential V_{dip}

$$V_{dip}(\vec{r}) = -\vec{d} \cdot \vec{E}(\vec{r}) \propto \alpha(\omega) |\vec{E}(\vec{r})|^2 \quad (7)$$

where $\alpha(\omega)$ is the polarizability of an atom and $I(\vec{r}) \propto |\vec{E}(\vec{r})|^2$ corresponds to the intensity of the laser light field. Hence, the optical dipole potentials proportional to the intensity and inversely proportional to the detuning Δ between the laser frequency ω and the resonant frequency of the atoms ω_0 (further details in [6] and [7]). For trapping purposes, the laser is tuned far away from any atomic resonance in order to be able to neglect resonant excitations and hence to have a purely conservative dipole interaction. For blue detuning, that is to say when $\omega > \omega_0$, Δ is positive, and so the potential is repulsive. Contrarily, a red detuned laser light, with $\Delta < 0$, generates an attractive potential and traps the atoms at the maximum of intensity.

Optical lattice

In order to simulate a condensed matter system, a spatially periodic potential is needed. It can be achieved by overlapping two counter-propagating Gaussian laser beams which will interfere and lead to a standing wave, the peaks and nodes of which will serve as a periodic trapping potential. Considering two beams propagating respectively along x and $-x$, the periodic trapping potential form is given by

$$V(r, x) = V_{lat} \sin^2(kx) e^{-\frac{2r^2}{w_0^2}} \quad (8)$$

where $V_{lat} = 4V_{dip}$ is the potential depth of the optical lattice resulting from constructive interference. The sinusoidal term establishes the periodicity of the lattice which is half the periodicity of the laser light, $k = 2\pi/\lambda$ being the wave vector of the laser light used to produce the lattice. The exponential term denotes the radial envelop given by a cylindrical symmetric Gaussian beam profile with a waist w_0 , here r is the radial coordinate. The potential depth is usually expressed in units of recoil energy $E_r = \hbar^2 k^2 / (2m)$, and can be varied by changing the intensity of the laser beam. The extension to three dimension is straightforward, forming a cubic lattice at the intersection of three orthogonal standing waves (see figure 1). The major strength of the so-formed optical lattice lies in the ease of adjusting the lattice parameters: the periodicity of the lattice is linked to the wavelength of the laser whereas the laser intensity controls the lattice depth.

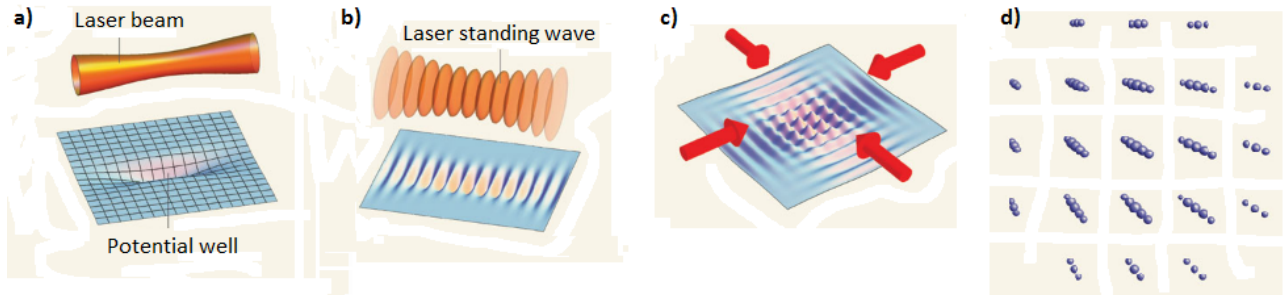


Figure 1: Potential landscape created by laser light and perceptible by the atoms. a) A light beam creates a potential, repulsive or attractive depending on the detuning, proportional to the light intensity b) Interference pattern created by two counter-propagating waves. c) Potential pattern created in two dimensions by a couple of counter-propagating waves d) In three dimensions, the attractive or repulsive points form a cubic lattice mimicking crystal sites [8]

2.3 Cold atoms in an optical lattice

Confining potential

Before being loaded into a lattice, the atoms are held in a dipole trap, the confinement of which is stronger than the confinement provided by the Gaussian profile shape of the counter-propagating lattice beams. The last one can therefore be neglected. Two beams create the dipole trap and remain

when the lattice beams are switched on. A beam propagating along x generates a strong confining potential along y and z and a weak one along x as shown on figure 1a. In fact, only two beams are necessary to create a confinement in the three directions and the confinement will be Stronger in the orthogonal direction of both laser beams. The external potential experienced by the atoms is therefore the sum of periodic lattice potential and of the confining dipole trap potential V_{conf} . Hence

$$V_{ext}(\vec{r}) = V_{conf}(\vec{r}) + V_{lat}(\vec{r}) \quad (9)$$

can be plugged into eq. 5.

Bloch and Wannier functions

In response to the potential periodicity in the Hamiltonian, the energy spectrum exhibits a band structure and, from Bloch's theorem [9], the eigenstates "Bloch wave functions" are plane waves whose amplitudes are modulated with the same periodicity as the lattice potential

$$\psi_{n,q}(r) = u_{n,q}(r)e^{iqr} \quad (10)$$

where $u_{n,q}(r + \pi/k) = u_{n,q}(r)$, q being the quasi-momenta and n the band index. However, Bloch wave functions are completely delocalized over all the lattice. Here, the regime of interest is given by the condensed matter tight-binding approximation meaning that the wave function of an electron becomes very small when at a distance bigger than the lattice constant. In other words, each electron is tightly bound to its nuclei and not shared over the lattice [9]. It is therefore more convenient to introduce an orthogonal and normalized set of wave functions which are localized at individual lattice sites. The so-called Wannier functions describing well a localised atom in the n^{th} energy band can be expressed as a function of the Bloch wave functions as

$$w_n(r - r_i) = \frac{1}{\sqrt{N}} \sum_q e^{-iqr_i} \psi_{n,q}(r) \quad (11)$$

Here r_i is the position of the i^{th} lattice site and N is a normalization constant. Assuming that the condensate is adiabatically loaded into the optical lattice, i.e. the lattice potential is slowly ramped up in order to keep the energies resulting from this dynamic small compared to the excitation energies of the second band, only the ground state of the lattice will be populated. Hence, the field operator $\hat{\psi}(\vec{r})$ can be expressed in the lower band Wannier functions basis as following:

$$\hat{\psi}(\vec{r}) = \sum_i \hat{a}_i w(\vec{r} - \vec{r}_i) \quad (12)$$

\hat{a}_i being the annihilation operator for the i^{th} lattice site.

The Bose-Hubbard model

Plugging eq. 12 into eq. 5 leads to the Bose-Hubbard Hamiltonian describing atoms in an optical lattice

$$\hat{H} = -J \sum_{\langle i,j \rangle} \hat{a}_i^\dagger \hat{a}_j + \sum_i (\epsilon_i - \mu) \hat{n}_i + \sum_i \frac{1}{2} U \hat{n}_i (\hat{n}_i - 1) \quad (13)$$

where $\hat{n}_i = \hat{a}_i^\dagger \hat{a}_i$ corresponds to the number of bosons on the i^{th} lattice site. As the Wannier functions are localized on one lattice site in particular, only the on-site interaction and the tunneling with the nearest neighbors are considered, which is why the first term is summed over nearest neighbors $\langle i,j \rangle$ and the two last terms over a single site i .

The first term of the Bose-Hubbard Hamiltonian is the hopping term. J describes the tendency of the

atoms to tunnel from one potential well to a neighboring one and therefore tends to delocalize each atom over the lattice sites.

$$J = - \int w(\vec{r} - \vec{r}_i) \left(-\frac{\hbar^2}{2m} \nabla^2 + V_{lat}(\vec{r}) \right) w(\vec{r} - \vec{r}_j) d\vec{r} \quad (14)$$

The second term is simply linked to the external confinement, $\epsilon_i = V_{conf}(\vec{r}_i)$ being the offset energy. The chemical potential μ is introduced to fix the mean number of particles in the system.

The last term describes the on-site interaction. U is the repulsive on-site interaction and corresponds to the energy that would need to be added to the system in order to have two atoms in the lattice well instead of only one.

$$U = (4\pi\hbar^2 a_s/m) \int |w(\vec{x})|^4 d^3x \quad (15)$$

U , in opposition to J tends to localize the atoms on one lattice site.

Superfluid to Mott insulator: a quantum phase transition

At this point, it can already be foreseen that the behavior of the system will be strongly related to the ratio between U and J . Because there are two competing energy scales, there will be two different ground states separated by a quantum phase transition: a superfluid ground state, in which the condensate is delocalized over the lattice sites if the tunneling J is the dominant parameter, and a insulating ground state presenting only one atom per site if the on-site interaction U is higher. Hence, as shown in figure 2 the system will undergo a quantum phase transition from a superfluid to a Mott insulator as the depth of the lattice is increased.

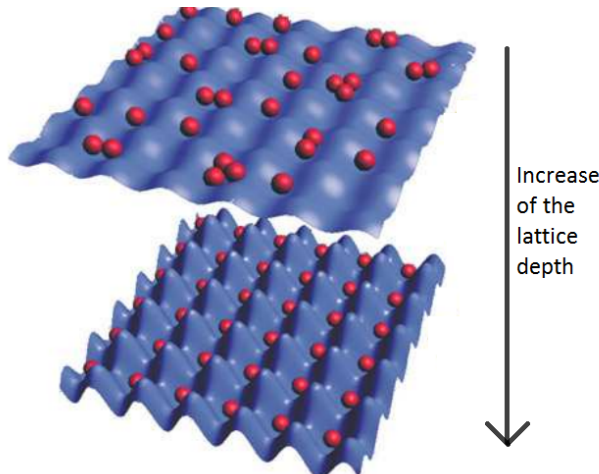


Figure 2: Phase transition from superfluid to Mott insulator. As the lattice depth increases, the ratio J/U becomes smaller and smaller, and the energy of the system is minimized if the atoms adopt a configuration of one atom per well [10]

2.4 Prospective experiments

The main goal of the BEC IV team is to work on various forms of quantum magnetism. In particular, spin gradient demagnetization cooling and tilted optical lattice leading to antiferromagnetic-like ordering are the two main experiments that are waiting to be done. In both of these experiments, a reliable and easily tunable magnetic field gradient is required.

Spin gradient demagnetization cooling

Spin gradient demagnetization cooling [4] [5] is linked to a transfer of energy from some degree of freedom of the system to another. The system considered is a BEC, loaded into a three-dimensional optical lattice in the presence of a weak magnetic field gradient where the atoms are prepared in a mixture of two distinct hyperfine states. Two hyperfine states correspond to two different magnetic moments. The gradient will therefore pull the atoms toward opposite sides of the trap. Thus, two spin domains will be created with a mixed region in between, the size of which will depend on the magnetic field gradient. At zero-temperature, the boundary between the two spin regions would be perfectly sharp. The system is initially prepared applying a given magnetic field gradient, if the gradient is then reduced adiabatically, the mixed spin region will get larger, storing more entropy. Knowing that the entropy of the system, considered isolated, remains constant, this excess of entropy must be extracted from other degrees of freedom. This entropy redistribution decreases the temperature of the whole system.

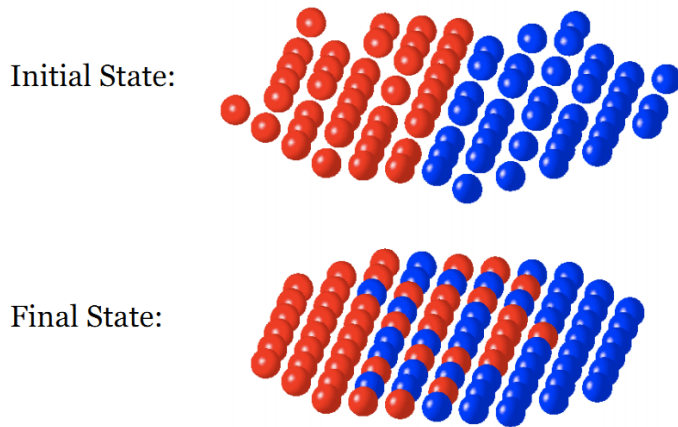


Figure 3: Gradient demagnetization cooling. In the initial state, the magnetic field gradient is strong and, therefore, the spins are perfectly ordered in two domains. As the gradient is lowered adiabatically, the energy of the system will flow from other degrees of freedom, like thermal agitation, into spin excitation. The system will thus be cooled. [11] [12]

Tilt experiment

The magnetic properties of condensed matter systems are important to study, theoretically speaking as well as regarding the technological applications. Using a Bose-Einstein condensate trapped in an optical lattice as described above, the transition between different magnetic ordering found in condensed matter systems can be simulated and studied. For example, the transition between paramagnetic phase, where all spins point in the same direction, and the antiferromagnetic phase characterized by alternation of spin up and spin down, can be reproduced by the transition between single site-occupation and the alternation of empty sites and two particles per site [1]. The Hamiltonian of the two systems are similar. If a decrease in temperature enables such a phase transition in condensed matter systems, it will be the increase of an applied magnetic field gradient which will play this role in the simulator. Indeed, considering a Mott insulator phase, the application of an inhomogeneous magnetic field across the lattice will shift the energy differently according with the position into the lattice. If the shift in energy between two neighboring site is higher than the on-site interaction energy, it will be favorable for the atom in the higher energy well to hop into the next site. If a constant and sufficiently strong magnetic gradient is applied to all the lattice, one over two atoms will hop leaving the system in a 0-2 occupation state. This equivalence is well illustrated by fig. 2 in [2], reproduced here in fig. 4.

We consider that we have one atom per well before any tilt. The addition of a constant magnetic

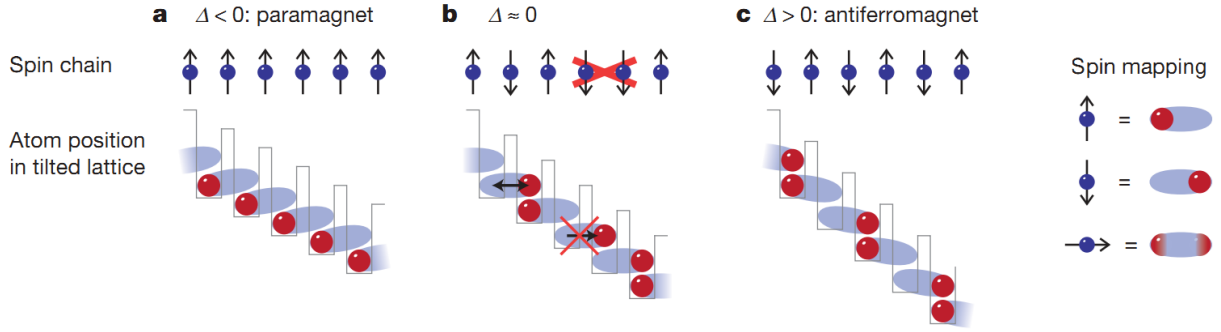


Figure 4: This figure illustrate the parallel between a spin chain undergoing a phase transition from a paramagnetic state to an antiferromagnetic state and atoms in an optical lattice, which reorder when the shift in energy E due to the magnetic field become degenerate with the repulsion energy U of two particles in the same well. a) When $\Delta = E - U < 0$, the occupancy is one atom per site, which is equivalent to all the spin in the same direction. b) The transition happens when $\Delta = 0$ as the energy degeneracy is reached. c) Then, as $\Delta > 0$, one over two atoms hop to the next well, mapping a spin flip and leading to the equivalent of an antiferromagnet. [2]

field gradient will then tilt the optical lattice along this gradient. The gradient must be direct in the (1,1,1) direction because we want to have a 3d chessboard pattern. Let us consider the 2d picture, if the gradient is along (1,0) we will get a line with 2 atoms per well followed by a line with no atoms then another line with 2 atoms per well and so on, which is the reason that the gradient must be along (1,1). Once this system is achieved experimentally, the creation of the antiferromagnetic phase can be studied as well as the size of the domains containing this order, which is to say the correlation length of this system. To see how this order is destroyed when the gradient is lower would also be interesting.

3 Simulation and requirement on the magnetic field

To realize such experiments, a configuration with eight coils is chosen: a pair of anti-Helmholtz coils to create a gradient and three pairs of Helmholtz coils to create a three-axis bias field in order to direct the gradient. This section will explain the reasons for and the details of such a configuration, as well as the strength of the field required. This discussion will be supported by numerical simulations realized with Matlab.

3.1 Magnetic fields and choice of the coils configuration

The realization of the experiment described previously will set several conditions on the magnetic field that have to be applied in the chamber where the atoms sit. After a small reminder on magnetic fields, these requirements will be formulated

About magnetic fields

In order to create the magnetic field that can be used for the tilt of the optical lattice or for the spin thermometry experiment, magnetic coils are required. A steady current flows through the wire loops creating a static magnetic field. Biot-Savart's law allows one to calculate the strength and the direction of a magnetic field created by a current:

$$\vec{B} = \frac{\mu_0 I}{4\pi} \int \frac{d\vec{l} \times \vec{r}}{r^2} \quad (16)$$

where $\mu_0 = 4\pi \cdot 10^{-7} V \cdot s / A \cdot m$ is the vacuum permeability, $d\vec{l}$ is the infinitesimal length of conductor carrying electric current I and \hat{r} is the unit vector from the wire element to the point where the field is calculated. For a magnetic coil formed by N loops of wire, this equation can be solved analytically along the axis of the coil, namely x .

$$B_x = \frac{\mu_0}{4\pi} \frac{2\pi R^2 IN}{(x^2 + R^2)^{3/2}} \quad (17)$$

where R is the radius of the coil, x is the distance from the center of the coil to the point on the x -axis where the field is calculated.

Limitations of the previous configuration

The magnetic field gradient applied to the atoms in the optical lattice needs to be homogeneous and smoothly tunable in any direction. The coils currently used on the machine, namely two coils creating the gradient along the vertical axis and two pairs of coil on both horizontal axis, present some major problems slowing down the achievement of the experiments described earlier. Indeed, the spin gradient demagnetization cooling has already been done with the BEC IV machine, leading to a measured temperature as low as 1nK [3], but the non-homogeneity of the magnetic field gradient was a limiting factor toward lowest temperatures. The coils creating the bias field are small and distant, leading to a strong curvature of the field in the region of interest. This lack of homogeneity results into a non precise direction of the gradient over the space at really weak magnetic field gradients. The gradient cannot easily be decreased until very small values along one specific axis. It will have a component along the other axes which cannot be neglected when the amplitude of the gradient approaches zero. The tilted lattice experiment cannot be achieved with the coils already in place because the gradient they produce is not strong enough to favor an even number of atom per well. Higher gradient and better homogeneity are therefore two parameters that need to be taken into account in the design of new coils.

Homogeneity and Helmholtz configuration

To enable the experiments discussed above, the magnetic field must be homogeneous over the spatial region occupied by the atoms. This region is not more than one micron large in each direction of the space. Using a pair of identical coils resting on the same axis and with current flowing in the same direction, one can find out the optimal distance between them in order to minimize the magnetic field variation along their axis, namely x . A Taylor expansion around $x=0$, corresponding to the mid plane of the coils, can be written

$$B(x) = B(0) + \left. \frac{\partial B}{\partial x} \right|_{x=0} \cdot x + \left. \frac{\partial^2 B}{\partial x^2} \right|_{x=0} \cdot x^2 + O(x^3) \quad (18)$$

Due to the symmetry about the mid-plane, $B(x)$ is an even function so $\left. \frac{\partial B}{\partial x} \right|_{x=0}$ is null. The next term contributing the most is the second order term. To minimize the variation of $B(x)$, $\left. \frac{\partial^2 B}{\partial x^2} \right|_{x=0}$ must be set to zero. This condition is fulfilled when the distance d between the coils equals the radius of the coils R . This configuration is called the Helmholtz configuration. [13] Figure 5 shows simulations of the profile of the magnetic field along the axis of two identical coils for different configurations.

The same configuration, but with the current flowing in the opposite directions in the coils will be called anti-Helmholtz configuration and produce a magnetic quadrupole field, shown on figure 6. Indeed, according to Maxwell's equations, the divergence of the magnetic field must be zero. It leads to the fact that, as a magnetic gradient, for example pointing out, is created along the axis of the coils, two other gradients with half the amplitude and pointing in are also induced along the two other axes. It is an interesting feature because it means that with only one pair of coils in the anti-Helmholtz configuration, gradients are creating along three orthogonal axis. It is therefore useless to use anti-Helmholtz coils along the three axes.

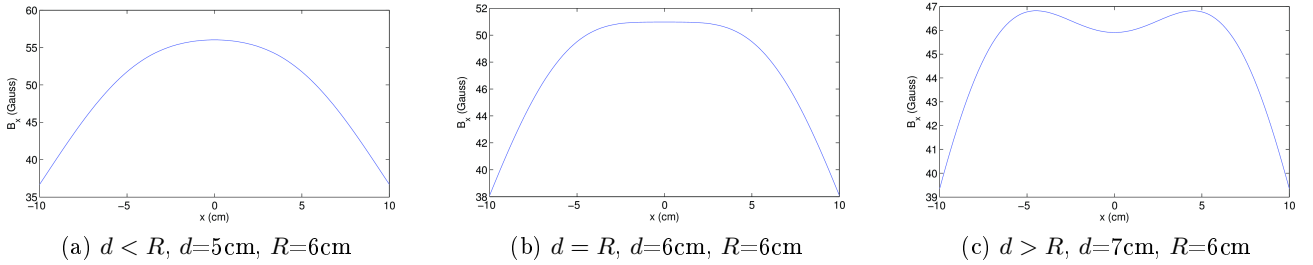


Figure 5: The amplitude of the magnetic field along the axis of the coils depends on the ratio between their radius R and the distance d between them. In the Helmholtz configuration (b), the region with constant magnetic field is larger than for other configurations: (a) and (c).

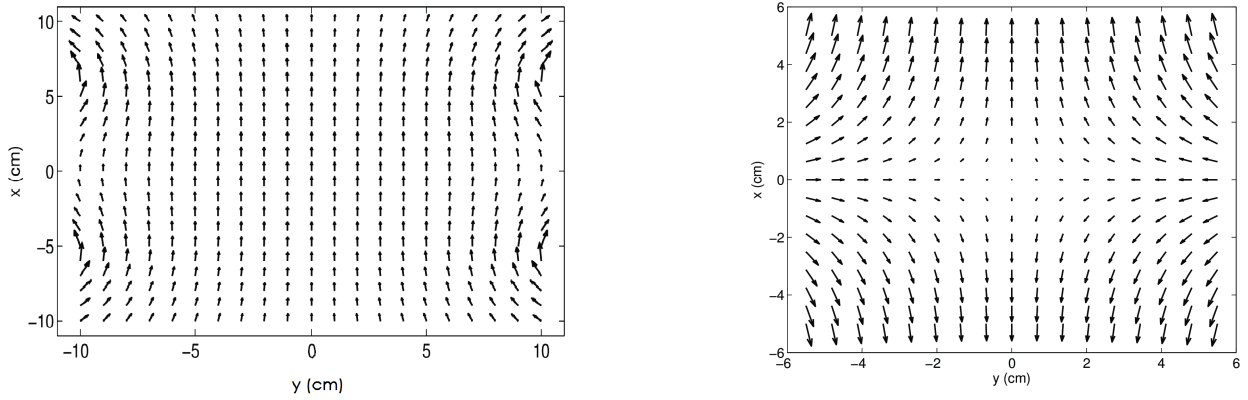


Figure 6: The left (right) plot shows the magnetic field created by a pair of coils in the Helmholtz (anti-Helmholtz) configuration , that is to say when the distance between the coils equals their radius and the current in each coil in flowing in the same direction (in opposite directions). The coils are at -6 and +6 cm along the x-axis, their diameter is therefore 24 cm.

Using three coils instead of only two, as in the Maxwell configuration, could provide a larger region with uniform magnetic field [14] but it would also block off the optical access to the science chamber, which must be preserved at any cost. Using more than three coils would become too space-consuming given the space available around the chamber.

A strong gradient is needed and this gradient must be able to point in any direction of the space. That is the reason why two coils in the anti-Helmholtz configuration will be positioned close to the chamber, creating a strong gradient, and then three other pairs of Helmholtz coils will be placed along the three orthogonal direction of space. This configuration of coils provide a good tuning.

New configuration

Given the number of mirrors, lenses and optical elements on the table (see appendix A), the free spaces for the coils are limited. Along the vertical axis, the two gradient coils can be arranged on top and under the science chamber, very closely to obtain a stronger gradient. The distance between the two coils have to be equal to their radius, that is to say about 12 cm. A few additional turns with independent inputs are added to create a bias field in the vertical direction. Concerning the horizontal axes, one needs to be careful. The bias coils mustn't block off the optical access to the chamber. For this reason, they will be placed further away from the chamber, respectively at about 13 and 14 cm from the center of the chamber. Their radii will therefore be respectively about 26 and 28 cm. Holders for the coils have also been designed. Four vertical aluminum bars with holes drilled at proper positions can provide a stable support for the coils, which will be subject to magnetic forces. A pair of bias coils

go through the optical table, which consequently need to be made *in situ*. Two semicircles made of plastic can be linked together through the table, forming a support for the coil. This support can then be rotated to wind the coil. The second pair of large bias coils can be made independently and simply added to the apparatus afterwards. They will also be held by the four aluminum rods as shown on the Solidworks design in figure 7. These aluminum rods can also support a platform for optics that help direct one laser beam creating the optical lattice. Indeed, in the current configuration of the experiment, these lenses are positioned at the end of a thin aluminum stick, which doesn't provide sufficient stability.

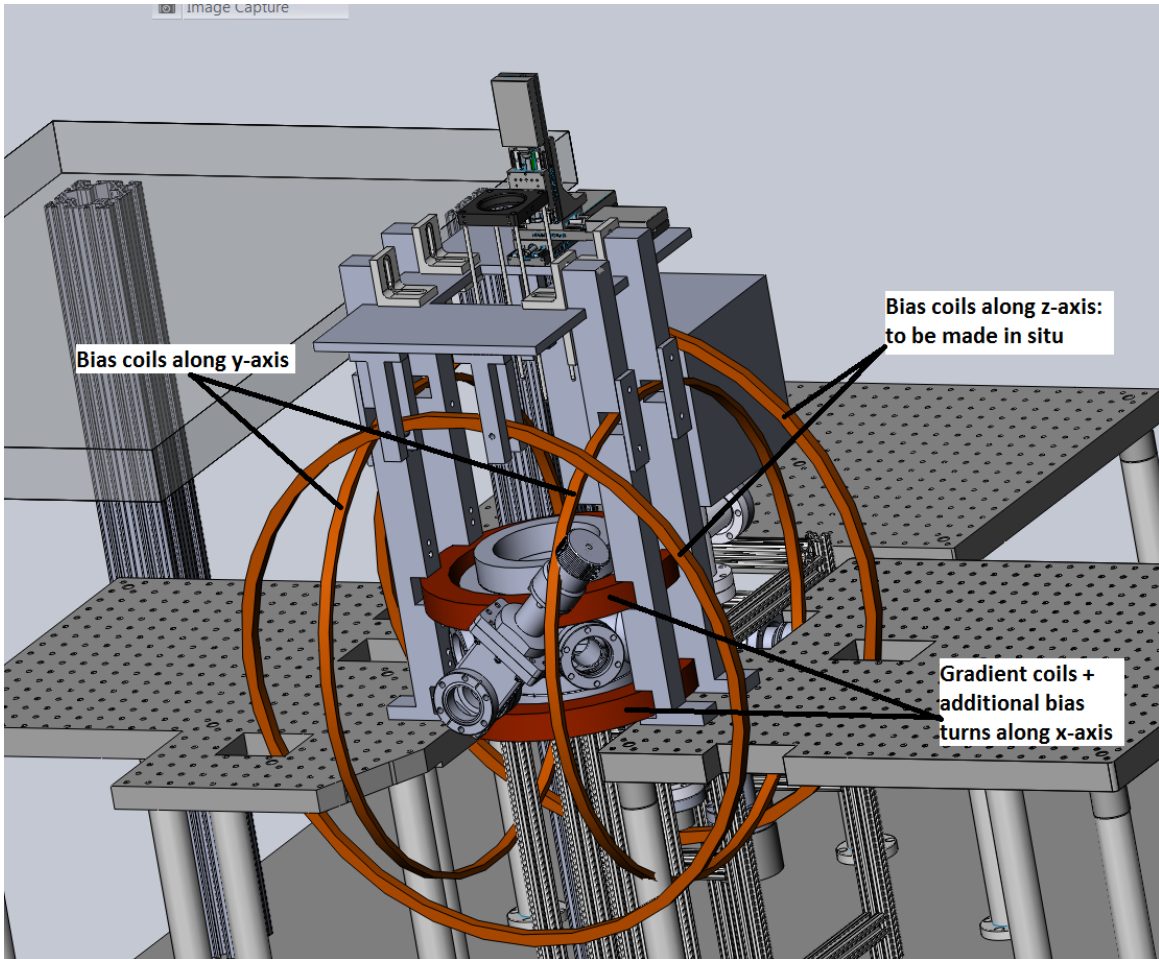


Figure 7: Drawing of the design of the magnetic coils around the science chamber. The two coils along the x-axis (vertical) serve to produce a strong magnetic field gradient in the chamber and the other coils the bias field. Aluminum holders are also designed to stabilize the coils and to enable winding the pair of coils along the z-axis *in situ*. A platform supporting optical elements is also added and will provide better stability for the optical path.

The radius of the coils is therefore a parameter that is fixed by the geometry of the apparatus. To create the magnetic field required for the experiments described previously, the number of turns and the current apply to the coils are still free parameters. To avoid the use of water-cooled coils, made of a hollow copper wire with cold water running inside, the current flowing through the coil shouldn't be too high. The kinds of power supplies available in the lab that could match with this requirement are a power supply delivering up to 75 Amperes and limited to 8Volts and another delivering 100A for 12V. The number of turns can then be determined, keeping in mind that more turns means more work winding them. Additionally, the coils shouldn't be bulky up to the point of blocking the windows of the science chamber. Thanks to a simulation of the magnetic field produced by the coils, one can

choose the optimum parameters combining satisfying magnetic field, suitable spacial positioning, bulk, and ease of production.

3.2 Numerical simulations

Given the configuration constraints of the coils, some code was written in order to determine the magnetic field produced by such coils as a function of the number of loops per coil and the current applied to them.

Preliminary study

As seen in section 3.1, the magnetic field produced by a coil can only be easily calculated analytically along its axis. To calculate the magnetic field over all space, one can approximate Biot-Savart's law given in eq. 16. Instead of integrating, the contributions $d\vec{B}_i$ to the magnetic field provided by every length element $d\vec{L}_i$ of the wire can be summed.

$$\vec{B} = \sum_{i=1}^n d\vec{B}_i = \sum_{i=1}^n \frac{\mu_0 I d\vec{L}_i \times \vec{r}_i}{4\pi R^2} \quad (19)$$

Depending on the number of parts the wire is divided into, this approximation will be more or less precise. To judge this precision, the approximated solution along the axis can be compared with the exact calculated by eq. 17

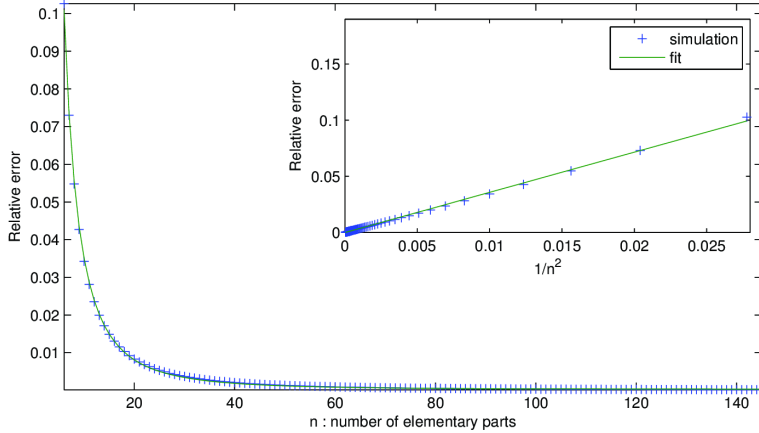


Figure 8: The relative error, which is the difference between the approximate value and the exact value of the magnetic field divided by the exact value, is plotted here in function of the number of elementary parts n . In the inset, the error is plotted versus $1/n^2$. The fit $y = 3.581 \cdot 1/n^2$ shows that the error converges as $1/n^2$.

The error converges to zero as $1/n^2$, and becomes smaller than 0.05% when n is bigger than 80. We considered this error negligible and therefore chose 100 steps in the further simulations with several pairs of coils.

Three dimensional simulation

The main goal of the program is to calculate the magnetic field and its gradient at each point in space, taking into account the contribution of the eight coils (two coils creating the gradient and two others on each axis x, y and z creating the bias field). This field gradient needs to be homogeneous over the region of interest, that is to say, where the atoms are trapped. The bias field will be created in all the three directions of the space by the three pairs of coils in the Helmholtz configuration. This will

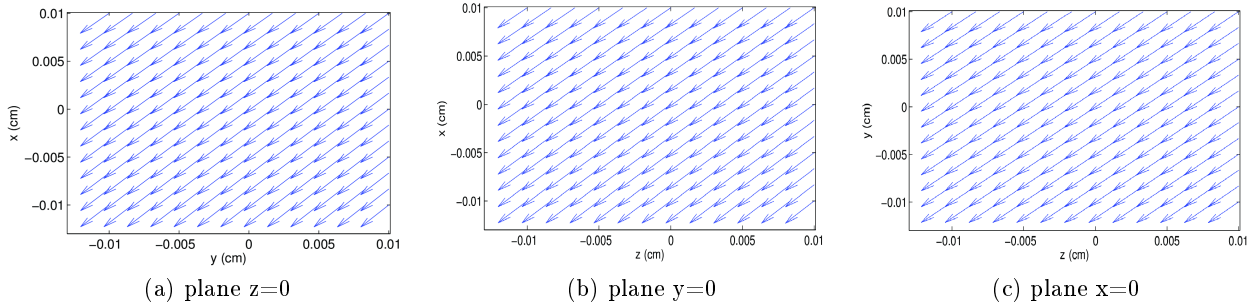


Figure 9: The direction of the gradient over the region of interest, one by one micron, is shown in the plane (a) $z=0$, (b) $y=0$, and (c) $x=0$. The length of the arrows, as well as their direction, are constant, it means that the gradient is constant over the spacial region of interest and points in the $(-1,-1,-1)$ direction, which is equivalent to the $(1,1,1)$ direction. These data were obtained setting a current of 18 A and 30 turns for the coils along the y-axis, 20 A and 30 turns for the coils along the z-axis, 100 A and 68 turns for the gradient coils and 15 A and 9 turns for the bias coils along x

also allow direction of the gradient where ever it is needed. Indeed, if a constant field is added to a quadrupole field configuration, the point of zero magnetic field is simply shifted in space. The zero field must be shifted out of the region of interest. All the calculations are based on the 1d approximate model: the coils are cut into small elements for which the corresponding magnetic field is calculated and then all the contributions are added. Before running the program, initial parameters need to be given for each coil: its radius, the number of loops, the position of its center and the intensity of the current that is flowing through it. The discretization step over the space in the three directions can also be chosen (see code in appendix C). The components B_x , B_y and B_z of the magnetic field are calculated for each coil and the total magnetic field is then obtained by adding the contribution given by each coil. The gradient can be calculated using the Matlab function which calculates the gradient of a vector field. This result can be verified by calculating the variation of each component of the magnetic field along an axis, for example along x, thanks to

$$\Delta B_x = \frac{B_{x+1} - B_x}{\Delta x} \quad (20)$$

Here B_x is the magnetic field at the position x and Δx is the distance between two discretization points along x. As the results are found to be similar, the Matlab function to calculate the gradient will be used. As the magnetic field is already a vector, taking the gradient of a vector will result in a 3x3 matrix. The gradient of the amplitude of the magnetic field, which is a vector with 3 components, will therefore also be calculated. The amplitude of the magnetic field is determined using

$$B = \sqrt{B_x^2 + B_y^2 + B_z^2} \quad (21)$$

Only the gradients along $(1,0,0)$, $(0,1,0)$ and $(0,0,1)$ have been calculated. However, to realize the tilted lattice experiment along the $(1,1,0)$ or $(1,1,1)$ axis, one can want to know the gradient of each component of the magnetic field along the $(1,1,0)$ and $(1,1,1)$ directions. Consequently, these gradients are determined as well using the magnetic field values along these two axes.

Several sets of parameters can be tried to see the behavior of the gradient. Figure 9 shows that the gradient can be directed along the $(-1, -1, -1)$ direction, which is what is ultimately wanted for the tilted lattice experiment.

3.3 Requirement on the magnetic field

Magnetic field gradient

To perform the lattice tilt in order to obtain the antiferromagnetic phase, the magnetic gradient needs to be strong enough that the energy it provides beats the on-site repulsion. To know the value of such a gradient, the on-site interaction must first be calculated. If the lattice is deep enough, that is to say for $V_{lat} > 10E_r$ [6], the Wannier function $w(\vec{x})$ can be approximated to the ground state of a harmonic oscillator

$$w(\vec{x}) = \left(\frac{m\omega}{\hbar\pi} \right)^{\frac{1}{4}} \exp\left(-\frac{m\omega x^2}{2\hbar}\right) \quad (22)$$

of frequency $\omega = 2\pi h\sqrt{n}/(m\lambda^2)$ where n , the number of recoils is taken equal to 15. This value is chosen because it is what is usually used in the experiment performed. This function is then plugged into eq. 15 and, knowing that the mass of the ^{87}Rb atoms is $1.4425400 \cdot 10^{-25} \text{ kg}$ and their scattering length $a_s = 103 a_0 = 5.45 \text{ nm}$ where $a_0 = 5.292 \cdot 10^{-11} \text{ m}$ is the Bohr radius [15], one can find the on-site interaction energy $U = 5.26 \cdot 10^{-31} \text{ J}$. This energy can also be expressed in term of frequency: $\nu_U = U/h = 794 \text{ Hz}$. Now, the gradient which provides an energy difference between two lattice sites equivalent to U can be found using the formula describing the Zeeman energy shift

$$E = \mu_B g_F m_F B \quad (23)$$

for an atom with a magnetic quantum number m_F and a Landé g-factor g_F in the hyperfine state F subject to a magnetic field B . Here $\mu_B = 9.27 \cdot 10^{-24} \text{ J} \cdot \text{T}^{-1} = h \cdot 1.40 \text{ MHz} \cdot \text{G}^{-1}$ is the Bohr magneton.

As magnetic field maxima in free space are not allowed by Maxwell's equations [16], only weak-field seeking states, for which $g_F m_F > 0$, can be trapped by static magnetic fields. However, in the science chamber, a optical trap is used so every state can be trapped. For ^{87}Rb atoms, the two states that will be used are $|F = 1, m_F = -1\rangle$ and $|F = 2, m_F = -2\rangle$, the absolute value of the g-factor g_F for these two states is $1/2$ [17].

If the equality between E and U is expressed in terms of frequency, it leads to $\nu_U = \mu_B g_F m_F B' d / h$ where d is the distance between two lattice sites and B' is the gradient of the magnetic field. Therefore, the gradient can be written as

$$B' = \frac{\nu_U}{\mu_B g_F m_F d} \quad (24)$$

where d will depend on the direction in which the gradient is pointing. The following table sums up the gradient amplitude needed to fulfill the previous condition in function of the direction chosen in the lattice

	State with $m_F = 1$	State with $m_F = 2$
direction (1,0,0) $d = 532 \text{ nm}$	$B' = 21.3 \text{ G/cm}$	$B' = 10.7 \text{ G/cm}$
direction (1,1,0) $d = \sqrt{2} \cdot 532 \text{ nm}$	$B' = 15.1 \text{ G/cm}$	$B' = 7.5 \text{ G/cm}$
direction (1,1,1) $d = \sqrt{3} \cdot 532 \text{ nm}$	$B' = 12.3 \text{ G/cm}$	$B' = 6.2 \text{ G/cm}$

This value is the magnetic gradient at the phase transition. A stronger gradient is therefore required to be in the antiferromagnetic phase.

Trapping potential due to the magnetic field

In the chamber, the atoms are subject to several forces, in other words, they are confined by several potentials. The magnetic field applied might influence the confinement of the atoms. To judge if the magnetic field will provide an extra-confinement to the cloud of atoms, its trapping frequency needs to be compared to the appropriate frequency. At the length scale of the cloud of atoms, the relevant

potential is the optical dipole trapping potential V_{ext} . The omega frequency of the optical trap have been measured experimentally and are $\omega_x = 150 \pm 10 Hz$ and $\omega_y = \omega_z = 50 \pm 10 Hz$. To determine the trapping potential induced by the magnetic field, one can start with a Taylor expansion along the transverse directions, for y and z small and setting x=0

$$\vec{B}(0, y, z) = \vec{B}(0, 0, 0) + \frac{\partial B_y}{\partial y} \Big|_{(0,0,0)} \cdot y + \frac{\partial B_z}{\partial z} \Big|_{(0,0,0)} \cdot z + O(y^2, z^2) \quad (25)$$

Maxwell's equation states that $\text{div} \vec{B} = 0$, which corresponds to $\frac{\partial B_x}{\partial x} + \frac{\partial B_y}{\partial y} + \frac{\partial B_z}{\partial z} = 0$. Thanks to the symmetry of the two coils in the anti-Helmoltz configuration, $B' \equiv \frac{\partial B_y}{\partial y} = \frac{\partial B_z}{\partial z} = -\frac{1}{2} \frac{\partial B_x}{\partial x}$. Along the x axis, only the x component of the magnetic field is non-null: $\vec{B} = B_x = B_0$. Therefore, eq. 25 can be rewritten as

$$\vec{B}(0, y, z) = B_0 \begin{pmatrix} 1 \\ 0 \\ 0 \end{pmatrix} + B' \begin{pmatrix} 0 \\ y \\ z \end{pmatrix} + O(y^2, z^2) \quad (26)$$

To calculate the magnetic energy, the norm of the magnetic field needs to be known using eq. 21

$$\begin{aligned} B &= \sqrt{B_0^2 + B'^2 y^2 + B'^2 z^2} \\ &= B_0 \left(1 + \frac{1}{2} \left(\frac{B'^2 y^2}{B_0^2} + \frac{B'^2 z^2}{B_0^2} \right) \right) \\ &= B_0 + \frac{1}{2} \frac{B'^2}{B_0} y^2 + \frac{1}{2} \frac{B'^2}{B_0} z^2 \end{aligned} \quad (27)$$

The energy experienced by the atoms due to the magnetic field, recalling eq. 23, is thus given by

$$E = \mu_B g_F m_F (B_0 + \frac{1}{2} \frac{B'^2}{B_0} y^2 + \frac{1}{2} \frac{B'^2}{B_0} z^2) \quad (28)$$

The terms in y^2 and z^2 can be seen as the curvature B'' of the magnetic trap, therefore $B'' = \frac{B'^2}{B_0}$. Considering B_0 as an offset, this energy has the same shape than the one of a harmonic oscillator

$$E = \frac{1}{2} K (y^2 + z^2) \quad (29)$$

Eq. 28 and 29 can thus be identified, and knowing that $K = m\omega^2$, the frequency of the trap created by the magnetic field can be found

$$\omega = \sqrt{\frac{\mu_B g_F m_F}{m} \frac{B'^2}{B_0}} \quad (30)$$

This frequency is linked to the value of the bias field B_0 and of the gradient B'

The bias field, in addition to enable directing the gradient, plays also a role in the magnetic confinement. As we don't want the magnetic field to add an extra-confinement on the cloud, the curvature of the magnetic potential needs to be smaller than the one of the optical dipole potential. It sets a constraint on the amplitude of the bias field. The minimum bias field required to avoid extra-confinement is given by

$$B_0 = B'^2 \cdot \frac{\mu_B g_F m_F}{\omega_{y,z}^2 m} \quad (31)$$

where the value for the optical trap frequency is taken to be the most constraining: $\omega_y = \omega_z = 40 Hz$. To be in the antiferromagnetic-like phase in the tilted lattice experiment, the gradient should be at least 25% higher than the limit gradient required to equal the on-site interaction U. The following table gives the limit gradient raised of 25% and the bias field corresponding to avoid an extra-confinement.

	State with $m_F = 1$	State with $m_F = 2$
direction (1,0,0)	$B' = 27 \text{ G/cm}$ $B_0 = 14.5 \text{ G}$	$B' = 13.5 \text{ G/cm}$ $B_0 = 3.7 \text{ G}$
direction (1,1,0)	$B' = 19 \text{ G/cm}$ $B_0 = 7.3 \text{ G}$	$B' = 9.5 \text{ G/cm}$ $B_0 = 3.5 \text{ G}$
direction (1,1,1)	$B' = 15.5 \text{ G/cm}$ $B_0 = 4.9 \text{ G}$	$B' = 8 \text{ G/cm}$ $B_0 = 2.6 \text{ G}$

The maximum bias field required is this 14.5 Gauss. Therefore, the bias coils along the x-axis need to provide a bias field of about 15 Gauss.

4 Construction and characterization of the coils

4.1 Choice of the wire

Resistance

The choice of the size of the wire is linked to the amount of current that will be flowing through it and of the length of it. Indeed, the power supplies can be used within a certain range of intensity and tension. The maximum intensity of the power supply has been an important parameter in the choice of the number of loops for each coil. The resistance of the coils can be calculated as following:

$$R = \frac{(2\pi N R_{coil} + 4)\rho_c}{\pi r^2} \quad (32)$$

where $\rho_c = 1.724 \cdot 10^{-8} \text{ ohm.m}$ is the electrical resistivity of the copper, R_{coil} is the radius of the coil, for the gradient coil $R_{coil} = 11.65 \text{ cm}$ and four meters of wire are added to take into account the link between the actual coil and the power supply, $N = 68$ is the number of loops, and r is radius of the copper wire. Knowing that $U = RI$, one can know the amount of current I that can be put into a coil with a given resistance depending on the limiting voltage U of the power supply. The radius r of the wire has been chosen to be able to use the power supply 100A-12V at its full power. If a copper wire with a radius $r = 1.632 \text{ mm}$, which corresponds to the gauge 8 of the american wires, is used, the resistance of the coil will be $R = 0.114 \text{ Ohm}$. However, only one of these power supplies is now available in the lab and two of them are required to run the coils. Another power supply delivering 75A and limited at 8V can be used but, due to the resistance of the coils, the intensity must not be tuned further than 65A. The power supplies for the bias coils doesn't need to provide that much current so a 20A/8V or 50A/8V power supplies can be used. The size of the wire can be smaller, for example, the gauge 12, with 2.053 mm in diameter may be used.

Heat study

It is also important to be sure that the coils won't heat too much, and eventually melt, during the experiment. The heat Q generated by the current I flowing through the coil of electrical resistance R , for the time t is given by Joule's law:

$$Q = I^2 \cdot R \cdot t \quad (33)$$

As more current flows in the gradient coils, they are the most likely to be over-heated, therefore the calculation will be made with their characteristics. In order to get an upper limit for the temperature variation, any kind of cooling can be neglected, and therefore, all the heat produced is assumed to be converted in a change of temperature of the copper wire. Using

$$Q = m \cdot c_m \cdot \Delta T \quad (34)$$

where $m = 3.8 \text{ kg}$ is the mass of the gradient coil, $c_m = 385 \text{ J} \cdot \text{kg}^{-1} \cdot \text{K}^{-1}$ is the mass-specific heat capacity of copper and ΔT corresponds to the change in temperature, the heating of the coil is therefore

estimated thanks to

$$\Delta T = \frac{I^2 \cdot R \cdot t}{m \cdot c_m} \quad (35)$$

If a current of 100A is switched on for $t = 10s$, the temperature will go up of $12^\circ C$, which will not affect the coil and don't require any cooling. Given the lifetime of the BEC in the science chamber, taking $t = 10s$ is an over-estimation, the current will probably flow into the coils for just few seconds. If the heating rate would have been too high, leading the copper to approach its melting temperature, water-cooled wire could have been used.

4.2 Final values for the parameters

In the following table will be summarize all the characteristics of the different coils.

Coils	Radius of the coil (cm)	Number of turns	Diameter of the wire (mm)	Resistance of the coil (ohm)
Gradient coils	11,65	68	3.264	0.114
Bias coils along x-axis	11.65	9	2.053	0.055
Bias coils along y-axis	26	30	2.053	0.276
Bias coils along z-axis	28	30	2.053	0.296

With these values, the bias field and the gradient produced are higher than what is required to do the experiment described above. However, it is always better to go as far as it is easily feasible because stronger gradients might be needed in further experiments and it would be worthwhile to have coils already in place which allow such experiments. Indeed, the gradient coil can provide a 50G/cm gradient along its axis, the bias coils produces a magnetic field up to 15 Gauss when the intensity of the current is $I = 20A$.

4.3 Details about the construction

Coil winding

The coils need to have 68 turns. Therefore, an alternation of layers with 9 and 8 turns can be repeated four times. Indeed, the wire has a circular section and, for this reason, it is easier to not have exactly the same number of turns per layer because the wire from the next layer will be tempted to go in between two turns of the previous layer to be closely packed. The coil is winded around a circular plastic support with has the right radius. The reel of copper wire is placed on an axis that will allows it to turn freely when the wire is pulled. The plastic support can be turned as well, enabling the winding. Before starting the winding, four plastic bands were placed along the support, in order to tighten the coil at the end of the winding. As the wire is rather thick, it is hard to bend to the appropriate shape. Therefore, a strong tension needs to be applied constantly while winding. After the first layer of nine turns has been done, wooden chock were clamped to keep the turns against each other and to help for the following layers. Once all the layers have been made, the plastics bands are tighten around the coils and the coil is removed from its support. Other plastic bands are added all around the coil to make sure it keeps its shape. Two identical coils are made this way. Their drawing and pictures can be found in Appendix B

Calibration

The calibration of the magnetic field has been made with a gaussmeter (FW Bell model 7030). It gives three values that correspond to the three component of the magnetic field at a given position. The two coils are positioned along the same axis at 11.65 cm away from each other. Then, a current of 2A, flowing in opposite direction in each coil, is applied. The probe of the gaussmeter is moved along the axis of the coils and the magnetic field is plotted versus the probe position. The values found are shown in figure 10 and compared with the numerically simulated field. The experimental result is in very good agreement with the simulation.

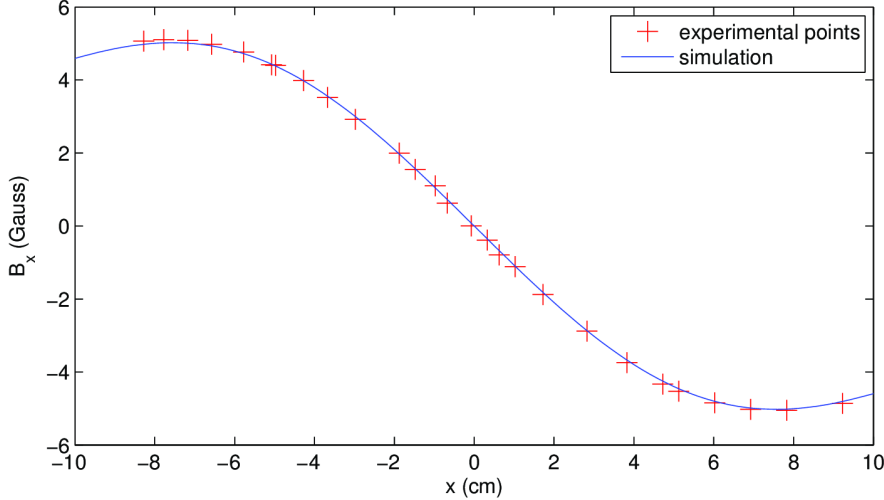


Figure 10: Comparison of the magnetic field measured and simulated for the gradient coils in the anti-Helmholtz configuration.

4.4 Characterization of the magnetic field in the science chamber

As long as the magnetic coils are away from the chamber, it is possible to characterize the magnetic field they produce with a probe, as we did just before. However, when placed around the chamber, the region where the atoms will sit is out of reach because a probe cannot be placed in the chamber under vacuum. In this situation, the atoms in the chamber can be used to probe the the magnetic field. The bias field can be determine by probing the energy difference between hyperfine levels due to the Zeeman effect. It can be done using RF frequencies.

To determine the gradient, the Stern-Gerlach experiment can be considered. Indeed, as the BEC is in the science chamber, applying the appropriate RF frequency will provide a mixture of two states: for example $|F = 1, m_F = 1\rangle$ and $|F = 1, m_F = -1\rangle$. Then, as the coils are switched on, the different states are accelerated in opposite directions due to their intrinsic angular momentum. Then by shinning light on the atoms after a certain time t , one can localize the two clouds and, by measuring the distance they have been deflected, know the strength and the direction of the magnetic gradient. Indeed, the force exerted by a magnetic field \vec{B} on a particle with magnetic moment $\vec{\mu}$ is:

$$\vec{F} = \nabla(\vec{\mu} \cdot \vec{B}) \quad (36)$$

$$= \pm \mu \nabla B \quad (37)$$

Using Newton's law:

$$\vec{F} = m \cdot \vec{a} = m \cdot \frac{\vec{v}}{t} = m \cdot \frac{\vec{d}}{t^2} \quad (38)$$

where \vec{a} is the acceleration, \vec{v} the velocity, and \vec{d} the displacement of the particles. A part of the atoms will be found at a distance d along the deflection axis and the other part at distance $-d$. Identifying eq. 36 and eq. 38, the magnetic field gradient can be expressed in function of the displacement:

$$\nabla B = \frac{m}{\mu} \frac{\vec{d}}{t^2} \quad (39)$$

Hence, the magnetic field can be determined in the vacuum chamber thanks to the magnetic properties of the atoms.

5 Conclusion

In this report, we discussed the optimum coils configuration around a vacuum chamber in which ultracold atoms experiments are performed. These experiments are carried out with atoms in a three-dimensionnal optical lattice and concern currently quantum magnetism. Two main experiments are planned: the tilted lattice experiment leading to the study of the antiferromagnetic ordering, and the spin gradient demagnetization cooling, going toward the lowest temperatures ever measured. Both experiments deal with ordering, which is a new road to explore in the domain of ultracold atoms. To achieve such experiments, a strong and constant gradient, as well as homogeneous bias fields to direct it are required. An improved coils configuration have been proposed. A pair of coils in the anti-Helmholtz configuration, at about 12 cm from each other, produces a strong gradient along the coils axis and a gradient with half this strength along the two other axes. Three pairs of coils in the Helmholtz configuration, one along each axis, create a homogeneous bias field that enables directing the gradient and plays a role in the magnetic confinement potential. The gradient required for these quantum magnetism experiments is 30 G/cm, and with the configuration chosen, this gradient can go up to 50 Gauss. The bias field needs to be 15 G, this value is reached furnishing a current of 20 A to the coils. Higher current would lead to higher bias fields. The two gradient coils have been made and characterized, they behave as expected by the simulations. These new coils, as well as the bias coils, might be placed around the chamber when the oven will be empty and need to be refilled. For now, the experiment is running and giving results, thus, to not to disturb the alignment and stop the taking of data, the update, which required to unmount optical elements, is delayed. However, when the new coils will be mounted, one can expect the achievement of new and interesting experiments.

References

- [1] Ian B. Spielman. Atomic physics: A route to quantum magnetism. *Nature*, 472:301, April 2011.
- [2] Jonathan Simon, Waseem S. Bakr, Ruichao Ma, M. Eric Tai, Philipp M. Preiss, and Markus Greiner. Quantum simulation of antiferromagnetic spin chains in an optical lattice. *Nature*, 472:307, April 2011.
- [3] David M. Weld, Patrick Medley, Hirokazu Miyake, David Hucul, David E. Pritchard, and Wolfgang Ketterle. Spin gradient thermometry for ultracold atoms in optical lattices. *Phys. Rev. Lett.*, 103(24):245301, Dec 2009.
- [4] Patrick Medley, David M. Weld, Hirokazu Miyake, David E. Pritchard, and Wolfgang Ketterle. Spin gradient demagnetization cooling of ultracold atoms. *Phys. Rev. Lett.*, 106(19):195301, May 2011.
- [5] David M. Weld, Hirokazu Miyake, Patrick Medley, David E. Pritchard, and Wolfgang Ketterle. Thermometry and refrigeration in a two-component mott insulator of ultracold atoms. *Phys. Rev. A*, 82(5):051603, Nov 2010.
- [6] Markus Greiner. *Ultracold quantum gases in three-dimensional optical lattice potentials*. PhD thesis, Ludwig-Maximilians-Universität München, 2003.
- [7] Rudolf Grimm and Matthias Weidem' Optical dipole traps for neutral atoms. volume 42 of *Advances In Atomic, Molecular, and Optical Physics*, pages 95 – 170. Academic Press, 2000.
- [8] Markus Greiner and Simon Folling. Condensed-matter physics: Optical lattices. *Nature*, 453(5):736, June 2008.
- [9] Neil W. Ashcroft and David N. Mermin. *Solid state physics*. Thomson Learning, Toronto, 1 edition, January 1976.

- [10] Juan Felipe Carrasquilla Alvarez. *The Bose-Hubbard model with disorder in low-dimensional lattices*. PhD thesis, Scuola Internationale Superiore di Studi Avanzati, 2010.
- [11] David Weld. Thermometry and cooling with ultracold spin mixtures. In *Towards Quantum Simulation*, 2010.
- [12] David M Weld and Wolfgang Ketterle. Towards quantum magnetism with ultracold atoms. *Journal of Physics: Conference Series*, 264(1):012017, 2011.
- [13] Thomas Tsz Ka Li. Tri-axial square helmholtz coil for neutron edm experiment. Master's thesis, Chinese University of Hong Kong, 2004.
- [14] Shouxian Zhang Sijiong Wang, Jian She. An improved helmholtz coil and analysis of its magnetic field homogeneity. *Review of Scientific Instruments*, 73:2175 – 2179, 2002.
- [15] P. S. Julienne, F. H. Mies, E. Tiesinga, and C. J. Williams. Collisional stability of double bose condensates. *Phys. Rev. Lett.*, 78(10):1880–1883, Mar 1997.
- [16] W. Ketterle and D. E. Pritchard. Trapping and focusing ground state atoms with static fields. *Applied Physics B: Lasers and Optics*, 54:403–406, 1992. 10.1007/BF00325386.
- [17] Daniel A. Steck. *Rubidium 87 D Line Data*. PhD thesis, Los Alamos National Laboratory.
- [18] Erik W. Streed, Ananth P. Chikkatur, Todd L. Gustavson, Micah Boyd, Yoshio Torii, Dominik Schneble, Gretchen K. Campbell, David E. Pritchard, and Wolfgang Ketterle. Large atom number bose-einstein condensate machines. *Review of Scientific Instruments*, 77(2):023106, 2006.
- [19] Laboratoire Kastler Brossel. La physique des atomes froids @ONLINE, June 2007.

Appendices

A Description of the apparatus for cooling

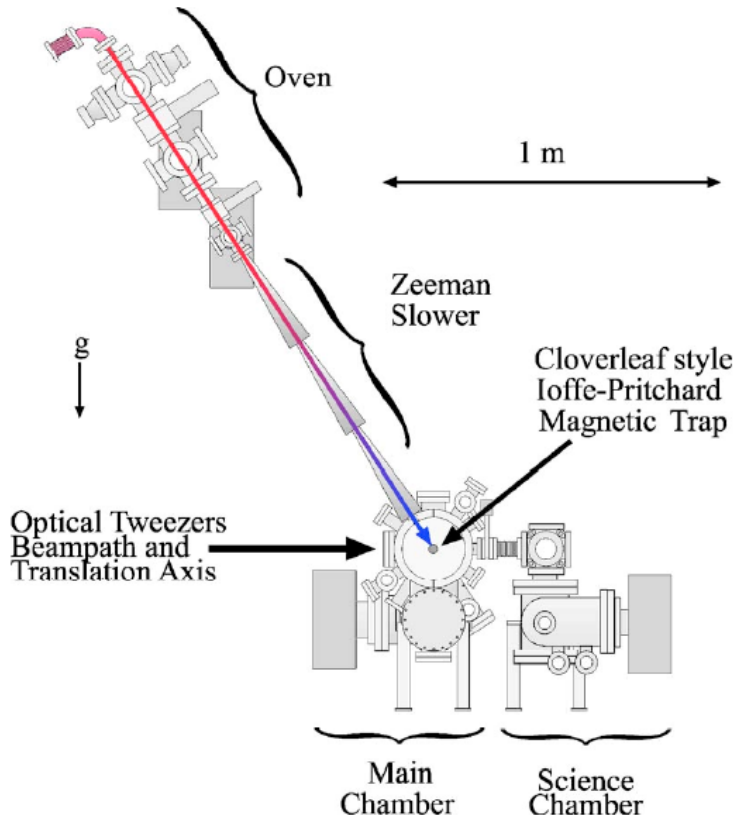


Figure 11: ^{87}Rb apparatus (schema from article[18])

In this appendix will describe succinctly and in a non exhaustive way the methods and the apparatus that create the BEC. A more detailed description of the apparatus and further information on cooling can be found in [18] and [19]. The cooling techniques depend on the properties of the atomic species chosen. The BEC4 machine shown on figures 11, 12 and 13 works with ^{87}Rb , it has only one electron in its outermost shell. A high vacuum (of the order of 10^{-11}) needs to be maintained in the two chambers to prevent any collision with the remaining gas particles. Everything starts in the oven. A rubidium source is heated up to $150\text{ }^{\circ}\text{C}$, creating a vapor of rubidium that will escape from the oven through a small hole, forming an effusive beam of atoms. This beam will go through the Zeeman slower whose aim is to slow down the atoms from an initial speed around 500 m/s to final speeds on the order of 10 m/s . The atoms are slow down thanks to resonant light. When an atom absorbs a photon, its momentum is changed by the momentum of the photon. If an atom of mass m absorbs a counter-propagating photon with momentum $\hbar k$, where k is the photon wavenumber, it recoils with a velocity $\hbar k/m$ to conserve the momentum. This recoil is also observed when the atom emits a photon. The aim is to slow down the atoms going into the main chamber with a high velocity. As the atoms have a certain velocity, they will experience a Doppler shift and see the light coming from the counter propagating laser beam with a different frequency. The frequency of the laser is therefore chosen to be smaller than the resonant frequency of the atom. Thereby the atoms propagating toward the main chamber will have more chance to absorb photons, thus to be slowed down, than the one going away from the chamber. A changing magnetic field is applied all along the path, in order to shift the energy levels of the atoms

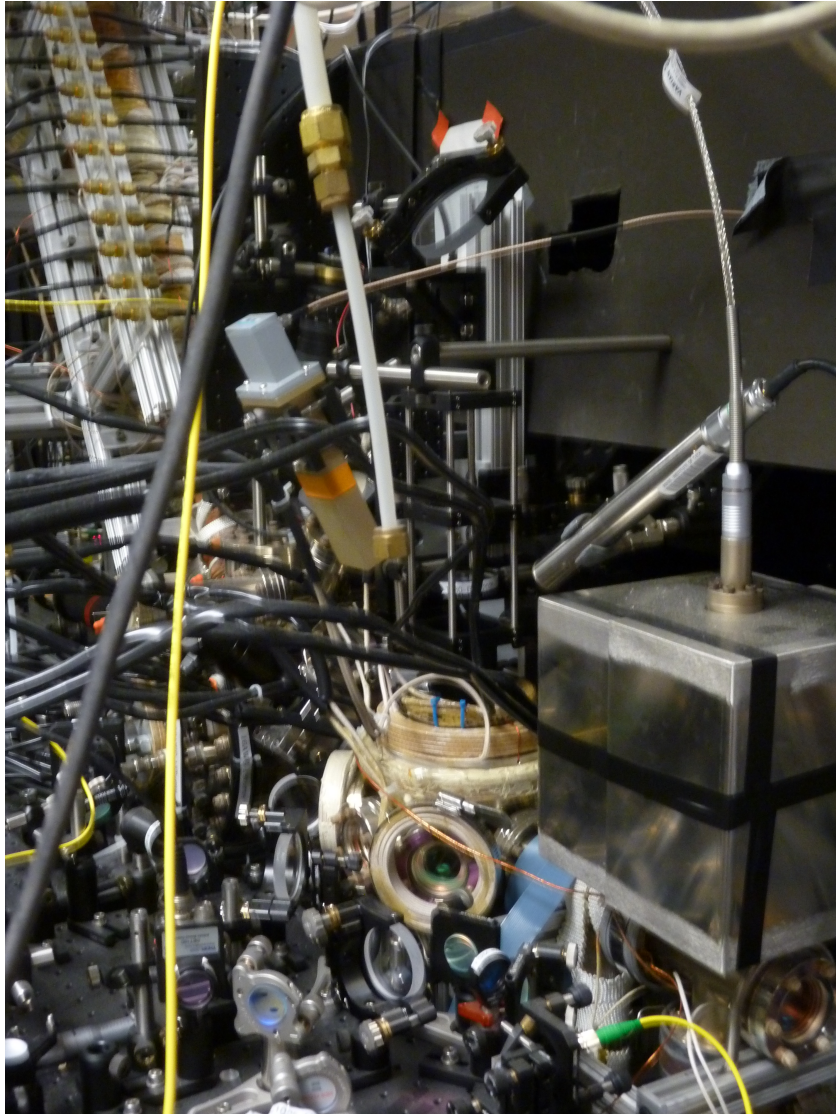


Figure 12: Picture of the apparatus used to cool and study ^{87}Rb atoms. The science chamber can be seen in the foreground and the Zeeman slower is visible in the background

and therefore change its resonant frequency, this will allows to maintain the resonance with the laser light. Like that, the atoms are slow down more and more as they travel through the Zeeman slower. The atoms are cooled further down in the optical molasses of the main chamber. When the recoil limit for cooling is reached, the evaporative cooling succeed to the optical cooling. The cloud of atoms is hold in a magnetic trap. RF frequencies flip the spin of the hotter atom and as, the atom is not in a trap state anymore, it escapes, taking with him more energy than the mean energy per atom. The RF-frequency is tuned in order to let escape cooler and cooler atoms. The other atoms left in the trap will rethermalize at a lower temperature. This cooling however leads to a loss in the atom number. Just before the transition from thermal gas to BEC, the atoms are transferred in the science chamber where they are cooled further down to cross the BEC phase transition. Once in the science chamber, the BEC can be trapped in an optical lattice and images can be taken thanks to a camera.

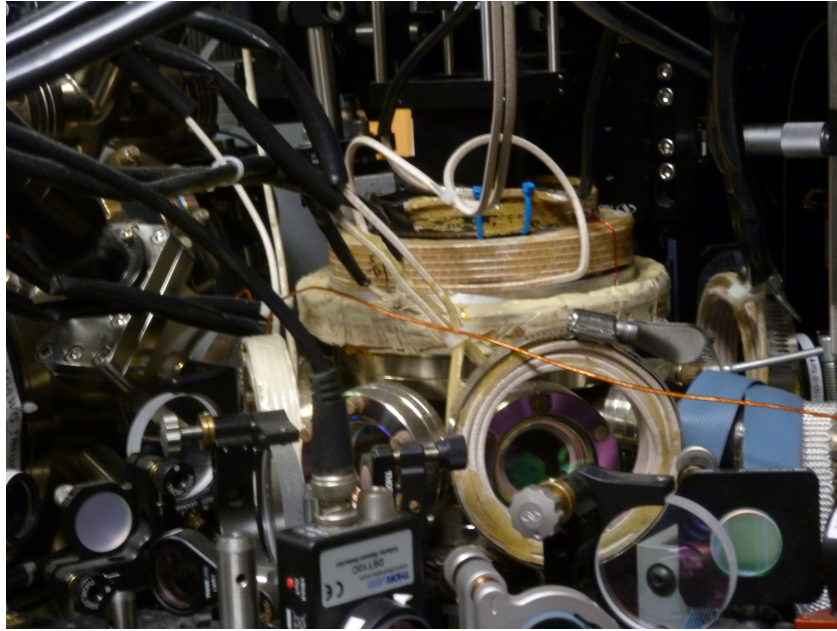


Figure 13: Science chamber with current coils configuration. The coils are not in an Helmholtz configuration and therefore, the magnetic field is not constant in the middle of the science chamber

B Gradient coils

B.1 Fabrication

This appendix section shows a picture of the realization of the gradient coils



Figure 14: Picture showing how the coils have been made. On the left sits the initial spool of copper wire and on the right, the black plastic support is turned to wind the coil around it. The pieces of wood clamped on the black support prevent the wire of expanding vertically.

B.2 Coils

This appendix section presents a picture and a technical drawing of a gradient coil realized.

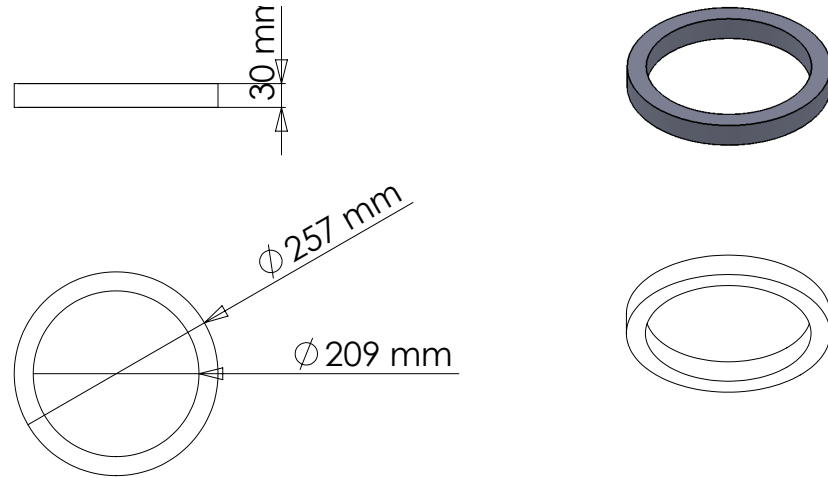


Figure 15: Technical drawing of a gradient coil. Two identical coils in the anti-Helmholtz configuration will produce the magnetic field

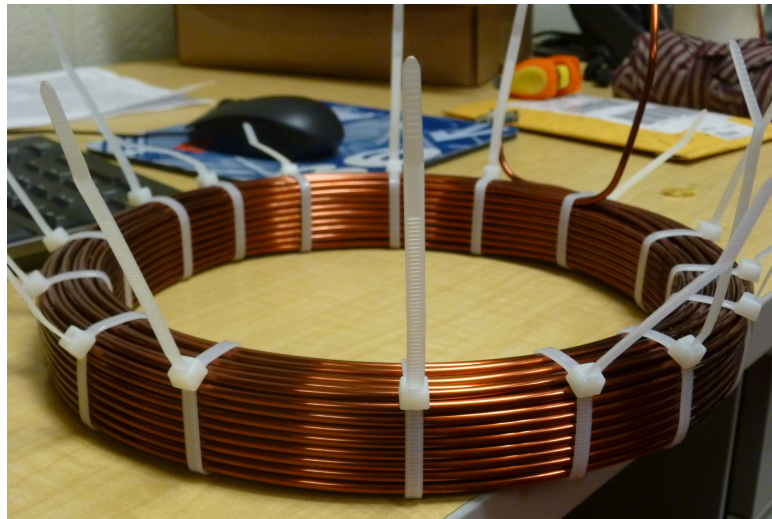


Figure 16: Picture of gradient coil. The coil is made of 68 turns of copper wire and the plastic bands help holding them together.

C Code to calculate the magnetic field

The codes calculating the magnetic field resulting from the new coil configuration is given here.

```
% This code enables to calculate the magnetic field, the gradient and the
% curvature created by coils along three orthogonal axes in the space.
% The parameters that can be change for each coil are: the number of turn
% N, the current flowing in the coil I, the radius of the coil R and the
% position of the coil x.
% 4 coils can be put on the x-axis, 2 on the y-axis and 2 on the z-axis.
% The length of the region over which the field will be calculated can also
% be chosen by x_Bmin and x_max as well as the number of elements the space
% will be divided in: nb_x_point.
% The number of piece in which the coil will be discretized to calculate
% the magnetic field, nb_theta_steps, can also be chosen. I advice to set
% at least nb_theta_steps = 60 for a good precision.
```

```
clear
format long

mu_0=4*pi*10^(-7);

%COILS ON THE X-AXIS
I_X1 = -100; % current running in coil 1 (X axis)
I_X2 = 100; % current running in coil 2 (X axis), if
              %sign(I_X1)≠sign(I_X2)=> anti-Helmoltz configuration
N_X1 = 68; % number of turns
N_X2 = 68;
R_X1= 0.12;
R_X2= 0.12; % radius of the coil 2
x_X1= -0.06; % x-position of the coil 1 of axis X
x_X2= 0.06;

I_X3 = 18;
I_X4 = 18;
N_X3 = 8;
N_X4 = 8;
R_X3= 0.12;
R_X4= 0.12; % radius of the coil 2
x_X3= -0.06; % x-position of the coil 1 of axis X
x_X4= 0.06;

% COILS ON THE Y-AXIS
I_Y1 = 20;
I_Y2 = 20;
N_Y1 = 26;
N_Y2 = 26;
R_Y1= 0.28;
R_Y2= 0.28;
y_Y1= -0.13;
```

```

y_Y2= 0.13;

% COILS ON THE Z-AXIS
I_Z1 = 20;
I_Z2 = 20;
N_Z1 = 30;
N_Z2 = 30;
R_Z1= 0.29;
R_Z2= 0.29;
z_Z1= -0.145;
z_Z2= 0.145;

x_Bmin = -0.11;
x_Bmax = 0.11;
y_Bmin = -0.11;
y_Bmax = 0.11;
z_Bmin = -0.11;
z_Bmax = 0.11;

nb_x_point = 22;           % !!! must be even !!!
nb_y_point = 22;           % !!! must be even !!!
nb_z_point = 22;           % !!! must be the same than nb_y_point !!!

x_step_size = abs(x_Bmin-x_Bmax)/nb_x_point;
y_step_size = abs(y_Bmin-y_Bmax)/nb_y_point;
z_step_size = abs(z_Bmin-z_Bmax)/nb_z_point;

nb_theta_steps = 100;        % numbers of theta steps for one turn
                            %(2*pi)
d_theta = 2*pi/nb_theta_steps;
length_dl_X=2*R_X1*tan(d_theta/2);    % length of dl expressed in function
                                         % of d_theta
length_dl_Y=2*R_Y1*tan(d_theta/2);
length_dl_Z=2*R_Z1*tan(d_theta/2);

Mat_dB_X = zeros(3,nb_theta_steps);

for zz = 1 : nb_z_point+1
    z_B(zz) = z_Bmin + (zz-1)*z_step_size;
    for yy = 1 : nb_y_point+1
        y_B(yy) = y_Bmin + (yy-1)*y_step_size;
        for xx = 1 : nb_x_point+1
            x_B(xx) = x_Bmin + (xx-1)*x_step_size;

            for ii = 1 : nb_theta_steps
                theta(ii) = (ii-1)*d_theta;

                dl_X = [0; -sin(theta(ii)); cos(theta(ii))];
                % dl : unit vector in the direction of dl
                r_X1 = [x_B(xx)-x_X1; y_B(yy)-R_X1*cos(theta(ii));
                        z_B(zz)-R_X1*sin(theta(ii))];      % vector r
                r_X1_hat = [x_B(xx)-x_X1; y_B(yy)-R_X1*cos(theta(ii));

```

```

z_B(zz)-R_X1*sin(theta(ii))]/norm(r_X1);
% unit vector r
r_X2 = [x_B(xx)-x_X2; y_B(yy)-R_X2*cos(theta(ii));
z_B(zz)-R_X2*sin(theta(ii))];
r_X2_hat = [x_B(xx)-x_X2; y_B(yy)-R_X2*cos(theta(ii));
z_B(zz)-R_X2*sin(theta(ii))]/norm(r_X2);
dB_X1 = mu_0*N_X1*I_X1*length_dl_X.*cross(dl_X,r_X1_hat)/(4*pi*(norm(r_X1))^2);
% Calculate infinitesimal contribution of dl
% to magnetic field thanks to Biot-Savart's law
dB_X2 = mu_0*N_X2*I_X2*length_dl_X.*cross(dl_X,r_X2_hat)/(4*pi*(norm(r_X2))^2);

r_X3 = [x_B(xx)-x_X3; y_B(yy)-R_X3*cos(theta(ii));
z_B(zz)-R_X3*sin(theta(ii))];
r_X3_hat = [x_B(xx)-x_X3; y_B(yy)-R_X3*cos(theta(ii));
z_B(zz)-R_X3*sin(theta(ii))]/norm(r_X3);
r_X4 = [x_B(xx)-x_X4; y_B(yy)-R_X4*cos(theta(ii));
z_B(zz)-R_X4*sin(theta(ii))];
r_X4_hat = [x_B(xx)-x_X4; y_B(yy)-R_X4*cos(theta(ii));
z_B(zz)-R_X4*sin(theta(ii))]/norm(r_X4);
dB_X3 = mu_0*N_X3*I_X3*length_dl_X.*cross(dl_X,r_X3_hat) /(4*pi*(norm(r_X3))^2)
dB_X4 = mu_0*N_X4*I_X4*length_dl_X.*cross(dl_X,r_X4_hat) /(4*pi*(norm(r_X4))^2)
Mat_dB_X(:,ii) = (dB_X1+dB_X2+dB_X3+dB_X4).* (10^4);
% storage of the results in a matrix, contribution of
% coil_X1 and coil_X2, *10^4 to have result in Gauss

r_Y1 = [x_B(xx)-R_Y1*sin(theta(ii)); y_B(yy)-y_Y1;
z_B(zz)- R_Y1*cos(theta(ii))];
r_Y1_hat = [x_B(xx)-R_Y1*sin(theta(ii)); y_B(yy)-y_Y1;
z_B(zz)- R_Y1*cos(theta(ii))]/norm(r_Y1);
r_Y2 = [x_B(xx)-R_Y2*sin(theta(ii)); y_B(yy)-y_Y2;
z_B(zz)- R_Y2*cos(theta(ii))];
r_Y2_hat = [x_B(xx)-R_Y2*sin(theta(ii)); y_B(yy)-y_Y2;
z_B(zz)- R_Y2*cos(theta(ii))]/norm(r_Y2);
dl_Y = [cos(theta(ii)); 0; -sin(theta(ii))];
dB_Y1 = mu_0*N_Y1*I_Y1*length_dl_Y.*cross(dl_Y,r_Y1_hat)/(4*pi*(norm(r_Y1))^2);
dB_Y2 = mu_0*N_Y2*I_Y2*length_dl_Y.*cross(dl_Y,r_Y2_hat)/(4*pi*(norm(r_Y2))^2);
Mat_dB_Y(:,ii) = (dB_Y1+dB_Y2).* (10^4);

r_Z1 = [x_B(xx)-R_Z1*cos(theta(ii));
y_B(yy)-R_Z1*sin(theta(ii)); z_B(zz)-z_Z1];
r_Z1_hat = [x_B(xx)-R_Z1*cos(theta(ii));
y_B(yy)-R_Z1*sin(theta(ii)); z_B(zz)-z_Z1]/norm(r_Z1);
r_Z2 = [x_B(xx)-R_Z2*cos(theta(ii));
y_B(yy)-R_Z2*sin(theta(ii)); z_B(zz)-z_Z2];
r_Z2_hat = [x_B(xx)-R_Z2*cos(theta(ii));
y_B(yy)-R_Z2*sin(theta(ii)); z_B(zz)-z_Z2]/norm(r_Z2);
dl_Z = [-sin(theta(ii)); cos(theta(ii)); 0];
dB_Z1 = mu_0*N_Z1*I_Z1*length_dl_Z.*cross(dl_Z,r_Z1_hat) /(4*pi*(norm(r_Z1))^2);
dB_Z2 = mu_0*N_Z2*I_Z2*length_dl_Z.*cross(dl_Z,r_Z2_hat) /(4*pi*(norm(r_Z2))^2);
Mat_dB_Z(:,ii) = (dB_Z1+dB_Z2).* (10^4);

```

```

    end
    B_X=[sum(Mat_dB_X(:,1:nb_theta_steps),2)];
    % Sum over all dl which gives magnetic field in one point
    Mat_B_X_x(:,xx) = B_X;
    % Mat_grad_B_X_x=[gradient(Mat_B_X_x(1,:));
    % gradient(Mat_B_X_x(2,:)); gradient(Mat_B_X_x(3,:))];
    B_Y=[sum(Mat_dB_Y(:,1:nb_theta_steps),2)];
    Mat_B_Y_x(:,xx) = B_Y;
    B_Z=[sum(Mat_dB_Z(:,1:nb_theta_steps),2)];
    Mat_B_Z_x(:,xx) = B_Z;

    end

x_B_prime=x_B(2:nb_x_point+1)

Mat_B_X_xy(:,:,yy) = Mat_B_X_x;
Mat_B_Y_xy(:,:,yy) = Mat_B_Y_x;
Mat_B_Z_xy(:,:,yy) = Mat_B_Z_x;

end
Mat_B_X_xyz(:,:,:zz) = Mat_B_X_xy;
Mat_B_Y_xyz(:,:,:zz) = Mat_B_Y_xy;
Mat_B_Z_xyz(:,:,:zz) = Mat_B_Z_xy;
end

Mat_B = Mat_B_X_xyz+Mat_B_Y_xyz+Mat_B_Z_xyz;
Mat_Bx(:,:, :) = Mat_B(1,:,:,:);
Mat_By(:,:, :) = Mat_B(2,:,:,:);
Mat_Bz(:,:, :) = Mat_B(3,:,:,:);

for zz = 1 : nb_z_point+1
    for yy = 1 : nb_y_point+1
        for xx = 1 : nb_x_point+1
            B_amplitude(xx,yy,zz)=sqrt(Mat_B(1,xx,yy,zz).^2 + Mat_B(2,xx,yy,zz).^2 + Mat_B(3,xx
        end
    end
end

%% Gradient of the amplitude of the magnetique field
% In David's code it is written:
% this odd order of gradient components is a result of the peculiar
% properties of MATLAB's gradient function.
% [gradBmagY gradBmagX gradBmagZ]=gradient(Bmag,x(2)-x(1),y(2)-y(1),z(2)-z(1));
% Therefore, I exchange Mat_grad_Bx and Mat_grad_By
[Mat_grad_By, Mat_grad_Bx, Mat_grad_Bz] =gradient(B_amplitude,x_step_size.*100,y_step_size.*100
% corresponds to the gradient of the amplitude of the Bfield

%% Gradient and curvature based on the amplitude of the vectors
for zz = 1 : nb_z_point+1
    for yy = 1 : nb_y_point+1
        for xx = 1 : nb_x_point+1
            Grad_B_amplitude(xx,yy,zz)=sqrt(Mat_grad_Bx(xx,yy,zz).^2 + Mat_grad_By(xx,yy,zz).^2

```

```

        % amplitude of the gradient of the amplitude of the Bfield
    end
end
end

[Mat_curv_By, Mat_curv_Bx, Mat_curv_Bz] =gradient(Grad_B_amplitude,x_step_size.*100,y_step_size

for zz = 1 : nb_z_point+1
    for yy = 1 : nb_y_point+1
        for xx = 1 : nb_x_point+1
            Curv_B_amplitude(xx,yy,zz)=sqrt(Mat_curv_Bx(xx,yy,zz).^2 + Mat_curv_By(xx,yy,zz).^2
        end
    end
end

%% Gradient in all the space along the three main axis
[My_grad_Bx, Mx_grad_Bx, Mz_grad_Bx]= gradient(Mat_Bx,x_step_size.*100,y_step_size.*100,z_step_size.*100);
% corresponds to the gradient of the x component of the Bfield, for example,
% My_grad_Bx corresponds to the variation of the x component of the Bfield
% along the y direction of the space
[My_grad_By, Mx_grad_By, Mz_grad_By]= gradient(Mat_By,x_step_size.*100,y_step_size.*100,z_step_size.*100);
% corresponds to the gradient of the y component of the Bfield
[My_grad_Bz, Mx_grad_Bz, Mz_grad_Bz]= gradient(Mat_Bz,x_step_size.*100,y_step_size.*100,z_step_size.*100);
% corresponds to the gradient of the z component of the Bfield

% Value of the gradient along the axis x (1,0,0)
Grad_Bx_100 = Mx_grad_Bx(:,(nb_y_point/2)+1,(nb_z_point/2)+1);
Grad_By_100 = Mx_grad_By(:,(nb_y_point/2)+1,(nb_z_point/2)+1);
Grad_Bz_100 = Mx_grad_Bz(:,(nb_y_point/2)+1,(nb_z_point/2)+1);

% Value of the gradient along the axis y (0,1,0)
Grad_Bx_010 = My_grad_Bx((nb_x_point/2)+1,:,:,(nb_z_point/2)+1);
Grad_By_010 = My_grad_By((nb_x_point/2)+1,:,:,(nb_z_point/2)+1);
Grad_Bz_010 = My_grad_Bz((nb_x_point/2)+1,:,:,(nb_z_point/2)+1);

% Value of the gradient along the axis y (0,0,1)
Grad_Bx_001 = Mz_grad_Bx((nb_x_point/2)+1,(nb_y_point/2)+1,:);
Grad_By_001 = Mz_grad_By((nb_x_point/2)+1,(nb_y_point/2)+1,:);
Grad_Bz_001 = Mz_grad_Bz((nb_x_point/2)+1,(nb_y_point/2)+1,:);

%% Curvature along the axis x (1,0,0), y (0,1,0) and z (0,0,1)
%In the x direction (1,0,0)
Curv_Bx_100 = gradient(Grad_Bx_100,x_step_size.*100);
Curv_By_100 = gradient(Grad_By_100,x_step_size.*100);
Curv_Bz_100 = gradient(Grad_Bz_100,x_step_size.*100);

%In the y direction (0,1,0)
Curv_Bx_010 = gradient(Grad_Bx_010,y_step_size.*100);
Curv_By_010 = gradient(Grad_By_010,y_step_size.*100);
Curv_Bz_010 = gradient(Grad_Bz_010,y_step_size.*100);

%In the z direction (0,0,1)

```



```

plot_grad_B_y0 = zeros(temp_size(1),temp_size(3));
plot_grad_B_z0 = zeros(temp_size(1),temp_size(2));

[X Y Z]=meshgrid(x_B,y_B,z_B);
% This is a copy of the gradient, set to zero everywhere off the XY, XZ,
% and YZ planes (for plotting purposes).
Mat_grad_Bx2=Mat_grad_Bx; Mat_grad_By2=Mat_grad_By; Mat_grad_Bz2=Mat_grad_Bz;
Mat_grad_Bx2(abs(X)&abs(Y)&abs(Z))=0;
Mat_grad_By2(abs(X)&abs(Y)&abs(Z))=0;
Mat_grad_Bz2(abs(X)&abs(Y)&abs(Z))=0;

figure(3);cla;clf;
subplot(2,3,1)
slice_ampli_xy = Grad_B_amplitude(:,:,nb_z_point/2)+1);
contourf(100.*x_B, 100.*y_B, slice_ampli_xy);
cb=colorbar;
ylabel(cb,'Gradient (G/cm)', 'FontSize',14);
set(cb,'FontSize',14);
xlabel('y (cm)'); ylabel('x (cm)');
title('amplitude of the gradient')

subplot(2,3,2)
slice_ampli_xz(:,:,:) = Grad_B_amplitude(:,(nb_y_point/2)+1,:);
contourf(100.*x_B, 100.*z_B, slice_ampli_xz);
cb=colorbar;
ylabel(cb,'Gradient (G/cm)', 'FontSize',14);
set(cb,'FontSize',14);
xlabel('z (cm)'); ylabel('x (cm)');
title('amplitude of the gradient')

subplot(2,3,3)
slice_ampli_yz(:,:,:) = Grad_B_amplitude((nb_x_point/2)+1,:,:);
contourf(100.*y_B, 100.*z_B, slice_ampli_yz);
cb=colorbar;
ylabel(cb,'Gradient (G/cm)', 'FontSize',14);
set(cb,'FontSize',14);
xlabel('z (cm)'); ylabel('y (cm)');
title('amplitude of the gradient ')

subplot(2,3,4)
[X1 Y1]=meshgrid(x_B,y_B);
plot11(:,:,)=Mat_grad_Bx(:,:,nb_z_point/2)+1);
plot12(:,:,)=Mat_grad_By(:,:,nb_z_point/2)+1);
h4=quiver(100.*X1,100.*Y1,plot12,plot11,1.4);
xlabel('y (cm)'); ylabel('x (cm)');
title('direction of the gradient (xy)')

subplot(2,3,5)
[X1 Z1]=meshgrid(x_B,z_B);
plot11(:,:,)=Mat_grad_Bx(:,:,nb_y_point/2)+1,:);
plot12(:,:,)=Mat_grad_Bz(:,:,nb_y_point/2)+1,:);
h3=quiver(100.*X1,100.*Z1,plot12,plot11,1.4);

```

```

xlabel('z (cm)'); ylabel('x (cm)');
title('direction of the gradient (xz)')

subplot(2,3,6)
[Y1 Z1]=meshgrid(y_B,z_B);
plot11(:,:,)=Mat_grad_By((nb_x_point/2)+1,:,:);
plot12(:,:,)=Mat_grad_Bz((nb_x_point/2)+1,:,:);
h5=quiver(100.*Y1,100.*Z1,plot12,plot11,1.4);
xlabel('z (cm)'); ylabel('y (cm)');
title('direction of the gradient (yz)')

ha = axes('Position',[0 0 1 1], 'Xlim',[0 1], 'Ylim',[0 1], 'Box','off', 'Visible','off', 'Units','normalized');
text(0.5, 1, '\bf Gradient of the amplitude of the magnetic field', 'HorizontalAlignment','center')

figure(75);cla;clf;
subplot(2,3,1)
slice_curv_xy = Curv_B_amplitude(:,:, (nb_z_point/2)+1);
contourf(100.*x_B, 100.*y_B, slice_curv_xy);
cb=colorbar;
ylabel(cb,'Curvature (G/cm^2)', 'FontSize',14);
set(cb,'FontSize',14);
xlabel('y (cm)'); ylabel('x (cm)');
title('amplitude of the curvature')

subplot(2,3,2)
slice_curv_xz(:,:,)= Curv_B_amplitude(:,(nb_y_point/2)+1,:);
contourf(100.*x_B, 100.*z_B, slice_curv_xz);
cb=colorbar;
ylabel(cb,'Curvature (G/cm^2)', 'FontSize',14);
set(cb,'FontSize',14);
xlabel('z (cm)'); ylabel('x (cm)');
title('amplitude of the curvature')

subplot(2,3,3)
slice_curv_yz(:,:,)= Curv_B_amplitude((nb_x_point/2)+1,:,:);
contourf(100.*y_B, 100.*z_B, slice_curv_yz);
cb=colorbar;
ylabel(cb,'Curvature (G/cm^2)', 'FontSize',14);
set(cb,'FontSize',14);
xlabel('z (cm)'); ylabel('y (cm)');
title('amplitude of the curvature ')

subplot(2,3,4)
[X1 Y1]=meshgrid(x_B,y_B);
plot11(:,:,)=Mat_curv_Bx(:,:, (nb_z_point/2)+1)
plot12(:,:,)=Mat_curv_By(:,:, (nb_z_point/2)+1)
h4=quiver(100.*X1,100.*Y1,plot12,plot11,1.4);
xlabel('y (cm)'); ylabel('x (cm)');
title('direction of the curvature (xy)')

subplot(2,3,5)

```

```

[X1 Z1]=meshgrid(x_B,z_B);
plot11(:,:,1)=Mat_curv_Bx(:,:,nb_y_point/2+1,:)
plot12(:,:,1)=Mat_curv_Bz(:,:,nb_y_point/2+1,:)
h3=quiver(100.*X1,100.*Z1,plot12,plot11,1.4);
xlabel('z (cm)'); ylabel('x (cm)');
title('direction of the curvature (xz)')

subplot(2,3,6)
[Y1 Z1]=meshgrid(y_B,z_B);
plot11(:,:,1)=Mat_curv_By((nb_x_point/2)+1,:,:)
plot12(:,:,1)=Mat_curv_Bz((nb_x_point/2)+1,:,:)
h5=quiver(100.*Y1,100.*Z1,plot12,plot11,1.4);
xlabel('z (cm)'); ylabel('y (cm)');
title('direction of the curvature (yz)')

ha = axes('Position',[0 0 1 1], 'Xlim',[0 1], 'Ylim',[0 1], 'Box','off', 'Visible','off', 'Units','normalized');
text(0.5, 1, '\bf Gradient of the amplitude of the gradient of the amplitude of the magnetic field');

figure(6);cla;set(gcf,'Color','white');set(gca,'FontSize',14);
slice(100.*X,100.*Y,100.*Z,Grad_B_amplitude,0,0,0); hold on;
h=quiver3(100.*X,100.*Y,100.*Z,Mat_grad_Bx2,Mat_grad_By2,Mat_grad_Bz2,'k','LineWidth',1.6); hold on;
cb=colorbar;
ylabel(cb,'Gradient (G/cm)', 'FontSize',14);
set(cb,'FontSize',14);
xlabel('y (cm)'); ylabel('x (cm)'); zlabel('z (cm)');
%caxis([0 .6]); % change or omit this for your own gradient range
axis tight;

% figure(34);cla;set(gcf,'Color','white');set(gca,'FontSize',14);
% h2=quiver3(100.*X,100.*Y,100.*Z,Mat_grad_Bx,Mat_grad_By,Mat_grad_Bz,'k','LineWidth',1.4); hold on;
% xlabel('x (cm)'); ylabel('y (cm)'); zlabel('z (cm)');
% title(' gradient')

Mat_B1(:,:,1)=Mat_B(1,:,:,(nb_z_point/2)+1);
Mat_B2(:,:,1)=Mat_B(2,:,:,(nb_z_point/2)+1);

figure(4);cla;clf;

[X1 Y1]=meshgrid(x_B,y_B);
h300=quiver(100.*X1,100.*Y1,Mat_B2,Mat_B1,'k','LineWidth',1.4); hold on
xlabel('y (cm)'); ylabel('x (cm)');
title('B field (xy)')

figure(1)
title('Magnetic field amplitude gradient direction')
subplot(3,3,1)
plot_grad_B_x0(:,:,1)= Mat_grad_Bx((nb_x_point/2)+1,:,:);

```

```

surf(y_B*100,z_B*100,plot_grad_B_x0); % *100 to have it in cm
xlabel('y (cm)'); ylabel('z (cm)'); zlabel('dB_x');
subplot(3,3,2)
plot_grad_B_x0(:,:,1)= Mat_grad_By((nb_x_point/2)+1,:,:);
surf(y_B*100,z_B*100,plot_grad_B_x0);
xlabel('y (cm)'); ylabel('z (cm)'); zlabel('dB_y')
subplot(3,3,3)
plot_grad_B_x0(:,:,2)= Mat_grad_Bz((nb_x_point/2)+1,:,:);
surf(y_B*100,z_B*100,plot_grad_B_x0)
xlabel('y (cm)'); ylabel('z (cm)'); zlabel('dB_z')

subplot(3,3,4)
plot_grad_B_y0(:,:,1)= Mat_grad_Bx(:,(nb_y_point/2)+1,:);
surf(z_B*100,x_B*100,plot_grad_B_y0);
xlabel('z (cm)'); ylabel('x (cm)'); zlabel('dB_x')
subplot(3,3,5)
plot_grad_B_y0(:,:,2)= Mat_grad_By(:,(nb_y_point/2)+1,:);
surf(z_B*100,x_B*100,plot_grad_B_y0);
xlabel('z (cm)'); ylabel('x (cm)'); zlabel('dB_y')
subplot(3,3,6)
plot_grad_B_y0(:,:,3)= Mat_grad_Bz(:,(nb_y_point/2)+1,:);
surf(z_B*100,x_B*100,plot_grad_B_y0)
xlabel('z (cm)'); ylabel('x (cm)'); zlabel('dB_z')

subplot(3,3,7)
plot_grad_B_z0(:,:,1)= Mat_grad_Bx(:,:,1,(nb_z_point/2)+1);
surf(y_B*100,x_B*100,plot_grad_B_z0);
xlabel('y (cm)'); ylabel('x (cm)'); zlabel('dB_x')
subplot(3,3,8)
plot_grad_B_z0(:,:,2)= Mat_grad_By(:,:,1,(nb_z_point/2)+1);
surf(y_B*100,x_B*100,plot_grad_B_z0);
xlabel('y (cm)'); ylabel('x (cm)'); zlabel('dB_y')
subplot(3,3,9)
plot_grad_B_z0(:,:,3)= Mat_grad_Bz(:,:,1,(nb_z_point/2)+1);
surf(y_B*100,x_B*100,plot_grad_B_z0);
xlabel('y (cm)'); ylabel('x (cm)'); zlabel('dB_z')

```

figure(2)

```

subplot(2,3,1)

plot_B_x0(:,:,1)= B_amplitude((nb_x_point/2)+1,:,:);
surf(y_B*100,z_B*100,plot_B_x0);
xlabel('y (cm)'); ylabel('z (cm)'); zlabel('B(G)');
title(sprintf('amplitude of the field and of the gradiant \n I_g_r_a_d=%d A N_g_r_a_d=%d turn'));
```



```

subplot(2,3,2)
plot_B_y0(:,:,1)= B_amplitude(:,(nb_y_point/2)+1,:);
```

```
surfc(z_B*100,x_B*100,plot_B_y0);
xlabel('z (cm)'); ylabel('x (cm)'); zlabel('B(G)'); title('');

subplot(2,3,3)
plot_B_z0(:,:,)= B_amplitude(:,:,nb_z_point/2)+1;
surfc(y_B*100,x_B*100,plot_B_z0);
xlabel('y (cm)'); ylabel('x (cm)'); zlabel('B(G)'); title('');

subplot(2,3,4)
plot_B_x0(:,:,)= Grad_B_amplitude((nb_x_point/2)+1,:,:);
surfc(y_B*100,z_B*100,plot_B_x0);
xlabel('y (cm)'); ylabel('z (cm)'); zlabel('dB(G/cm)')

subplot(2,3,5)
plot_B_y0(:,:,)= Grad_B_amplitude(:,(nb_y_point/2)+1,:);
surfc(z_B*100,x_B*100,plot_B_y0);
xlabel('z (cm)'); ylabel('x (cm)'); zlabel('dB(G/cm)')

subplot(2,3,6)
plot_B_z0(:,:,)= Grad_B_amplitude(:,:,nb_z_point/2)+1;
surfc(y_B*100,x_B*100,plot_B_z0);
xlabel('y (cm)'); ylabel('x (cm)'); zlabel('dB(G/cm)')
```